Tsunami Hazard Assessment of Point Roberts, Washington

Project Report

Draft of August 31, 2021

Randall J. LeVeque, Loyce M. Adams, and Frank I. González
University of Washington

Submitted to the Washington State Emergency Management Division
and Washington Geological Survey

Contents

1 Introduction

This report summarizes tsunami modeling results submitted to the Washington Geological Survey (WGS) in August, 2021, for use in the production of maximum inundation and current speed mapping products.

The study regions cover the coast of Point Roberts in Whatcom County from roughly longitude -123.14 to longitude -122.90 and latitude 48.94 to latitude 49.03 plus the coast around Semiahmoo Dr and Drayton Harbor in Whatcom County from roughly longitude -122.90 to longitude -122.69 and latitude 48.94 to latitude 49.03. Part of these regions lie in Canada. The region named Semiahmoo overlaps with part of what was called region N1 in the previous 2018–19 modeling project of Whatcom County [1], but now extends farther north of the region denoted N1 in that study.

At the time the previous project was performed, no fine-resolution topography was available for Point Roberts, and hence that portion of Whatcom County was omitted from the study. Moreover, the best coastal topography then available was the 3 arc-second British Columbia DEM [22], which only contains offshore bathymetry at 3" resolution and no onshore topography at all. Boundary Bay, which lies between Point Roberts and the US mainland, is very shallow and much of the land surrounding it is below MHW and protected by dikes. The lack of topography data in this region led to some uncertainty in the results presented for Region N1 in [1], as discussed in that report. The current modeling uses a new topography DEM developed in a collaboration between Ocean Networks Canada (ONC), other data providers in Canada, and the NOAA National Centers for Environmental Information (NCEI), as discussed further in Section 2.1.

In this report, in addition to modeling of Point Roberts, we also include some new modeling results of the Semiahmoo region, which overlaps the previous N1 region, and in particular includes Drayton Harbor. Some comparisons with the original model results have been performed in this area to assess the impact of the newly acquired topography; see Appendix C.

Both the Point Roberts and Semiahmoo regions extend north of latitude 49N into Canada, covering Tsawwassen, BC to the north of Point Roberts and the Semiahmoo First Nations land and some of White Rock, BC on the mainland. Inundation results on the Canadian side of the border will not be included in products produced by WGS, but these areas may be of interest to communities near the border. Note that recent Canadian modeling reports [10, 11] show modeling results south of the border, covering the east shore of Point Roberts and all of Drayton Harbor, so those results may also be of interest to US communities. When comparing the results, it is very important to note that the Canadian modeling is based on different tsunami sources (see Section 3.4), and so the two sets of results are complementary but not directly comparable.

We are currently engaged in collaboration with the Canadian tsunami modelers in an effort to compare the different numerical models being used for tsunami propagation and inundation, and also to perform a more extensive comparison of the different tsunami sources (hypothetical earthquakes) that have been used for hazard assessment.

In the Point Roberts region, we used one earthquake source from the Seattle Fault (SF-L), two from from the Cascadia Subduction Zone (CSZ-XL1, CSZ-L1), and one from the Alaska Subduction Zone (AKmaxWA). These sources are described in Section 3. This is a larger set of sources than was used for the original Whatcom County study [1], but is consistent with more recent studies [17, 15]. For the Semiahmoo region, only the CSZ-L1 source is considered here, for comparison with the previous results.

Results shown in this report include inundation depths and times of arrival that will be useful to coastal communities, as well as tsunami current speeds and momentum flux. GeoClaw Version 5.8.0 was used for the modeling [8].

Figure 1 shows the combined coastline studied, the union of two "fgmax regions" . For each fgmax region, GeoClaw results are provided for each considered earthquake. An fgmax grid is a fixed grid (fg) on which is saved the maximum (max) values of model variables attained during the duration of the simulation, including the fundamental variables water depth (h) and water speed (s) derived from the velocity components ($s = \sqrt{u^2 + v^2}$), as well as other quantities of interest derived from the depth (h) and horizontal momenta (hu and hv), the quantities modelled in the shallow water equations.

The combined fgmax points for the two regions of Figure 1 are shown in Figure 2. The fgmax points for region `PtRoberts` are shown separately in Figure 3 and those for region `Semiahmoo` in Figure 4. For region

`PtRoberts`, we modelled the CSZ-XL1, CSZ-L1, SF-L, and AKmaxWA sources. For region `Semiahmoo`, we only modelled the CSZ-L1 source.

For each of these 5 sets of results (4 events on region `PtRoberts` and 1 event on region `Semiahmoo`), the quantities of interest have been provided as netCDF files on a set of points with 1/3 arcsecond (1/3") spacing in both longitude and latitude (approximately 7 m and 10 m respectively). The data format is discussed further in Appendix A.

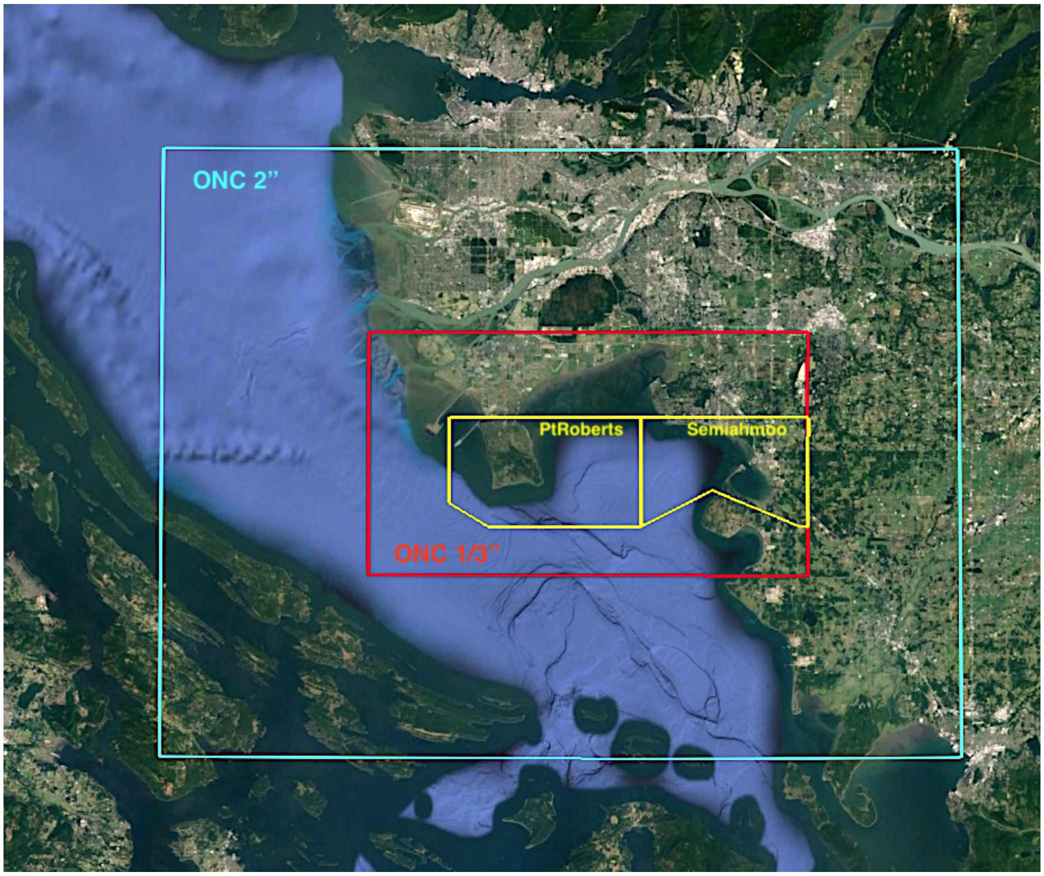

Figure 1: The yellow polygons show the two study regions considered in this project, and are shown in more detail in the following figures. The extents of the new high-resolution topography DEMs used in this area are also shown, and discussed further in Section 2.1. Imagery from Google Earth.

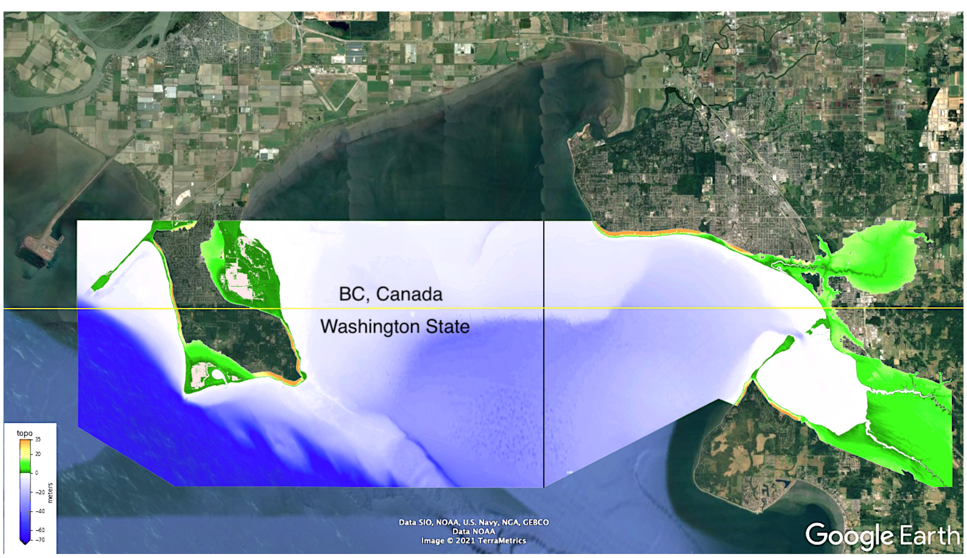

Figure 2: The combined fgmax points for regions `PtRoberts` and `Semiahmoo` are shown. The `PtRoberts` and `Semiahmoo` fgmax points are shown separately in the following two figures. Imagery from Google Earth.

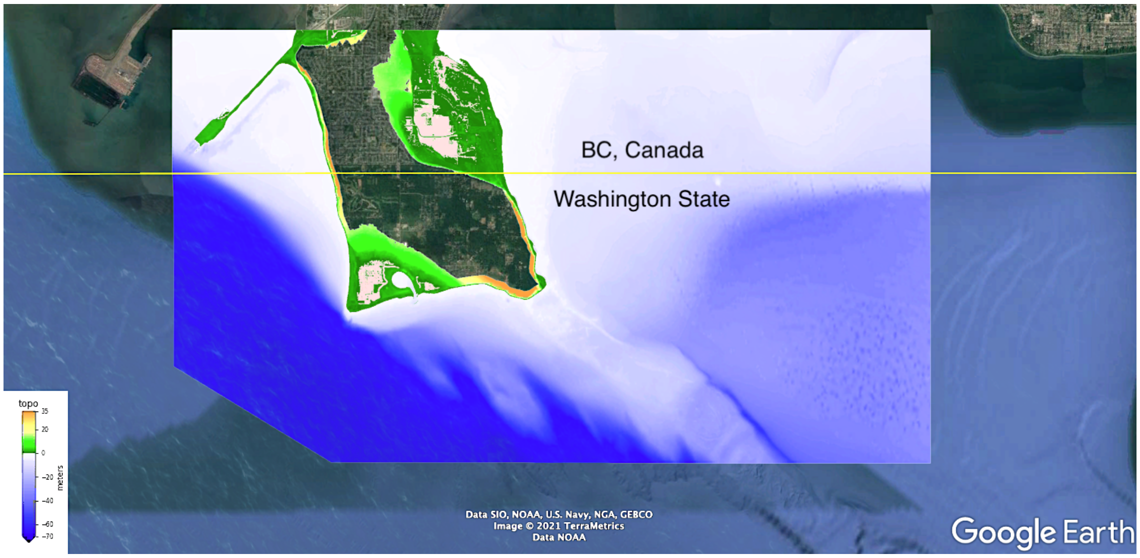

Figure 3: The colored regions show the fgmax points in the study region denoted `PtRoberts`, which extend up to 15 m elevation and some distance offshore. This fgmax region includes land in Point Roberts, WA and its coastline and overlaps with region `Semiahmoo` to its east. The region extends north of the border to cover Tsawwassen, BC as well. Points shaded pink show areas that are below MHW but that were identified as dry land (protected by dikes or levies) and initialized as dry in the simulations. Imagery from Google Earth.

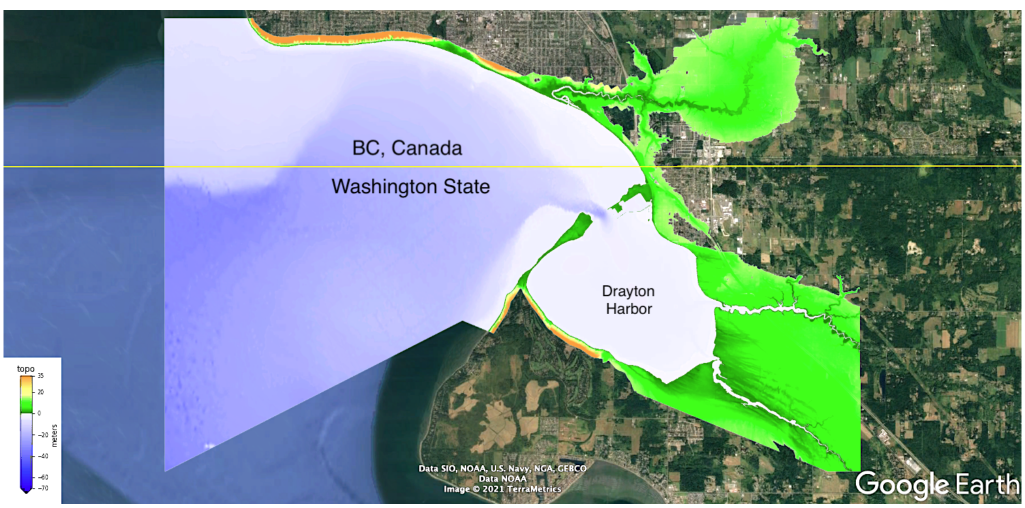

Figure 4: The colored regions show the fgmax points in the study region denoted `Semiahmoo`, which extend up to 15 m elevation and some distance offshore. This region includes Drayton Harbor, Blaine Harbor, the Semiahmoo Resort Golf Spa all in WA. Also included is the coastline along Peace Arch Provincial Park at the boundary of WA and Canada and coastline further north into Canada up to latitude 49.03. To this region's west is the region named `PtRoberts`. Imagery from Google Earth.

2 Topography and Bathymetry

All DEMs and project data utilize World Geodetic System 1984 (WGS84, ESPG:4326) as the standard coordinate system for this study. The fine-resolution coastal grids are referenced to Mean High Water (MHW).

Output from the model was requested at grid points spaced 1/3" in longitude and 1/3" in latitude, with the points aligned with cell centers of the 1/3" DEM files that are available for the coastal region. (Note that 1/3" in latitude is approximately 10.3 m. At this latitude, 1/3" in longitude is approximately 6.9 m). Topography at this resolution is needed covering the fgmax regions, but coarser topography can be used in regions that will only be covered by coarser computational grids.

GeoClaw uses finite volume methods with adaptive mesh refinement, and the finest grid resolution near regions of interest was set to the desired resolution of 1/3" by 1/3". It is important to note, however, that in the finite volume formulation the given DEM files are used to construct a piecewise bilinear function interpolating at the DEM points, and averages of this function over grid cells are then used as the topography values in the numerical method. Hence a cell that is centered at a DEM point overlaps 4 bilinear functions meeting at this point and the "GeoClaw topography" used in this grid cell will depend on the DEM values at 9 neighboring points. Moreover, if there is co-seismic subsidence (or uplift) in a cell the final GeoClaw topography value in this cell (which we denote by B) will include this deformation. For these reasons we provide both B and the DEM value Z at the same point in the netCDF files of model output, along with the co-seismic deformation dZ; see Appendix A.

2.1 Boundary Bay Topography and ONC DEMs

As mentioned in the Introduction, new topography has been used for this project that will be referred to as the ONC DEMs, which was developed in a collaboration between ONC and NCEI [24, 26]. These DEMs are at a spatial resolution of 1/9 arcsecond and cover Point Roberts and Drayton Harbor in the US, as well as all of Boundary Bay and farther north into British Columbia. These DEMs were modified by NCEI to reference them to MHW, and made available as a set of geotiff tiles covering rectangles 0.25 degrees on a side, consistent with other NCEI tiles in the database [9]. Note that the file names include the latitude and longitude of the NW corner of tile. The following 8 tiles were used for this project,

`onc19_n49x25_w123x50_2019v1_hwmt.tif`,

`onc19_n49x25_w123x25_2019v1_hwmt.tif`,

`onc19_n49x25_w123x00_2020v3_hwmt.tif`,

`onc19_n49x25_w122x75_2020v3_hwmt.tif`,

`onc19_n49x00_w123x50_2019v1_hwmt.tif`,

`onc19_n49x00_w123x25_2019v1_hwmt.tif`,

`onc19_n49x00_w123x00_2019v1_hwmt.tif`,

`onc19_n49x00_w122x75_2019v1_hwmt.tif`,

These tiles will eventually be published at [9].

Together these cover the rectangle $[-123.5,\ -122.5,\ 48.75,\ 49.25]$, shown in cyan in Figure 1. For this project, the DEM in this region was coarsened to 2". In addition, a cropped portion of this DEM was coarsened to 1/3" for fine-resolution modeling of the study regions. The 1/3" DEM covers the rectangle $[-123.24,\ -122.69,\ 48.9,\ 49.1]$ as shown in red in Figure 1, and covers all of Boundary Bay.

2.2 Other topography used

As in the previous Whatcom County study, the 1/3" Port Townsend DEM [20], Puget Sound DEM [23], and Strait of Juan de Fuca DEM [21] were coarsened to obtain 2" DEMs for use outside the regions covered by the 1/3" DEM. These DEMs are more efficient to use in GeoClaw on coarser grid levels where all the details of the 1/3" DEMs are not required.

The new ONC tiles do not cover all of the Canadian portion of the Salish Sea, and so the BC 3" DEM was still used over part of the Strait of Georgia north of the study region.

Outside of the study region, the Strait, and the Salish Sea, 1-minute topography for the Pacific Ocean and outer coasts was used from the global etopo1 dataset [3]. Note that this DEM is referenced to MSL but is only used away from the coastal regions of interest, and has a resolution that does not resolve coastal features enough for the vertical datum to matter.

The extents of all the DEMs mentioned above (except the 1-minute topo) are shown in Figure 5.

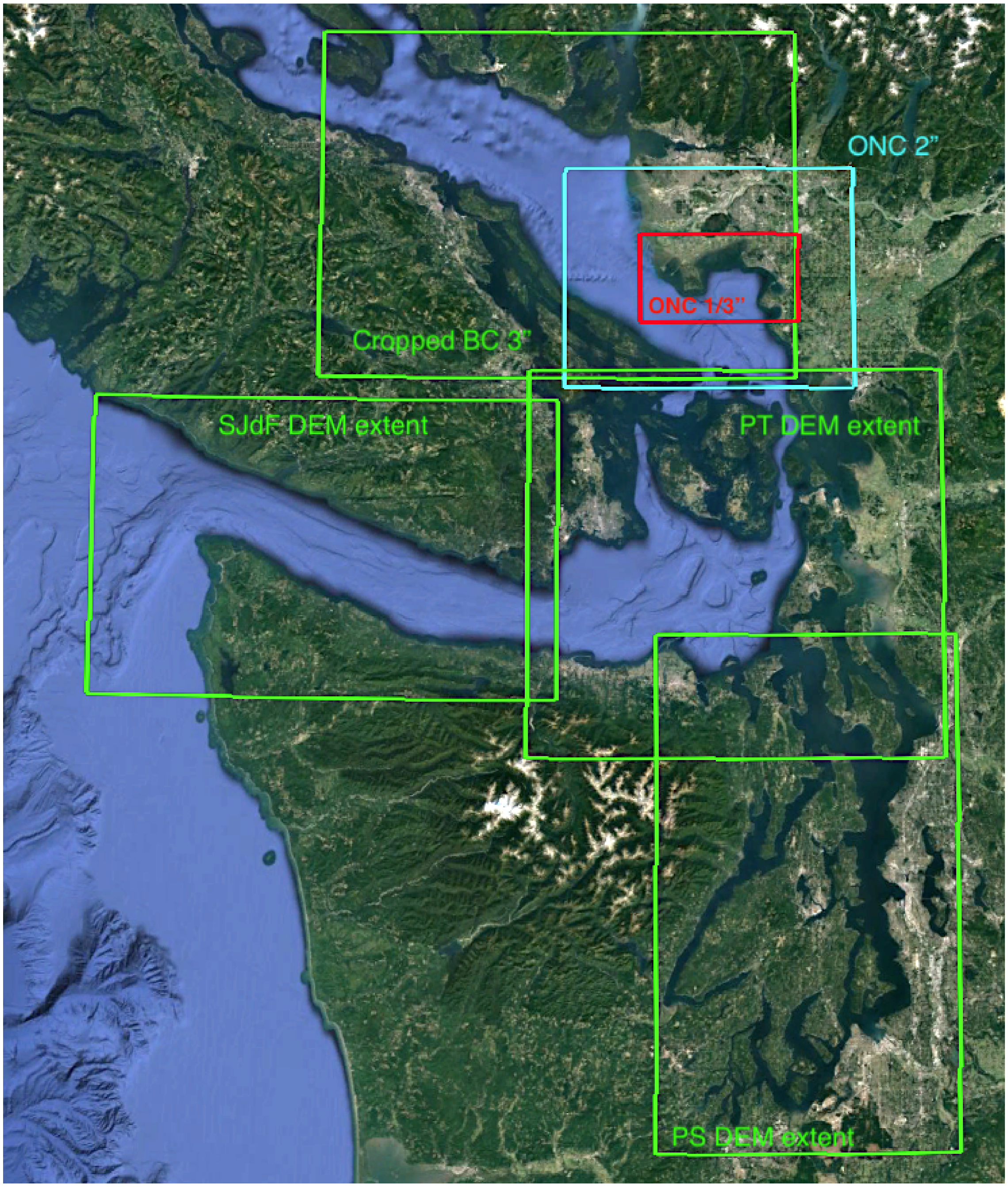

Figure 5: Green rectangles show the extent of the topography DEMs used in the previous Whatcom County study [1] that were again used in this work, as described in the text. The cyan rectangle shows the extent of the new ONC DEM that was coarsened to 2", and the red rectangle shows the extent of the new ONC DEM that was coarsened to 1/3", and that covers both study regions as shown in Figure 1. Imagery from Google Earth.

3 Earthquake Sources

Four earthquake sources were considered for the study of Point Roberts: a Cascadia Subduction Zone (CSZ) megathurst event with moment magnitude Mw 9.0 (denoted CSZ-L1), a larger CSZ event with moment magnitude Mw 9.1 (denoted CSZ-XL1), a potential Seattle Fault rupture denoted SF-L, and an Aleutian Subduction Zone event off the coast of Alaska with magnitude 9.24, denoted AKmaxWA.

Other potential sources have not been considered in this study. In particular the smaller Seattle Fault event SF-S that has been used in some past tsunami studies in Puget Sound was found to have negligible impact on Snohomish County in our previous work and would be even smaller in Whatcom County. There are also uncertainties associated with the proper specification of that fault, as discussed in [16]. Several other fault zones cross Puget Sound, but potential sources from these faults have not been considered.

3.1 Cascadia megathrust events CSZ-L1 and CSZ-XL1

The probability that an earthquake of magnitude 8 or greater will occur on the Cascadia Subduction Zone (CSZ) in the next 50 years has been estimated to be 10-14% (Petersen, et. al., 2002 [25]). The last such event occurred in 1700 (Satake, et al., 2003 [27]; Atwater, et al., 2005 [4]) and future events are expected to generate a destructive tsunami that will inundate Washington Pacific coast communities within tens of minutes after the earthquake main shock.

One potential CSZ event used in this study is the L1 scenerio developed by Witter, et al. (2013) [30]; crustal deformation for the region of interest is shown in Figure 6. The L1 source is one of 15 seismic scenarios used in a hazard assessment study of Bandon, OR, based on an analysis of data spanning 10,000 years. This scenario has been adopted by Washington State as the "maximum considered case" for many inundation modeling studies and subsequent evacuation map development; it is used because the standard engineering planning horizon is 2500 years and Witter, et al. [30] estimated that L1 has a mean recurrence period of approximately 3333 years, with the highest probability of occurrence of all events considered with magnitude Mw 9 or greater.

The original L1 source was developed for studies on the Oregon coast and was truncated at around 48N. An extension of this was developed by the NOAA Center for Tsunami Research (NCTR) group in the Pacific Marine Environment Laboratory (PMEL) in Seattle. The seafloor deformation is shown in Figure 6. As prescribed by the Washington Geological Survey (WGS), we used this extended source, the same version of the CSZ-L1 source as used in our other recent tsunami hazard assessments, [15, 16, 1, 29, 2].

For this study a larger magnitude CSZ event was also considered, the XL1 source that was originally developed for Witter, et al. [30] as a Mw 9.1 event with a splay fault. The sea floor deformation for XL1 was essentially the same as for L1 but magnified by a multiplicative factor of approximately 1.5 at each point. For this project we started with the PMEL extension of the L1 source and magnified it by the same factor in order to obtain a version of the XL1 source that also extends north to the north. The seafloor deformation is shown in Figure 6.

The CSZ-L1 and CSZ-XL1 events create very large waves along the outer coast and a substantial wave that propagates into the Strait of Juan de Fuca and into Puget Sound, affecting parts of the study regions in Whatcom County roughly 2 hours after the event (which is assumed to be instantaneous in our modeling). No subsidence or uplift is produced in Whatcom County from these events.

Simulations for the CSZ events were run out to 10 hours. The maximum water depth and speeds recorded at the fgmax points for these CSZ events typically occur between 2 and 4.25 hours post quake. The maximum water depth occurs with the first wave, but there are significant later waves up to about 8 hours after the earthquake, as seen in the gauge plots of Section 7.

3.2 Seattle Fault event SF-L

Figure 7 shows contours of uplift and subsidence due to a hypothetical event on the Seattle fault that we denote by SF-L. Earlier tsunami hazard studies have referred to this as a Mw 7.3 event. However, when we

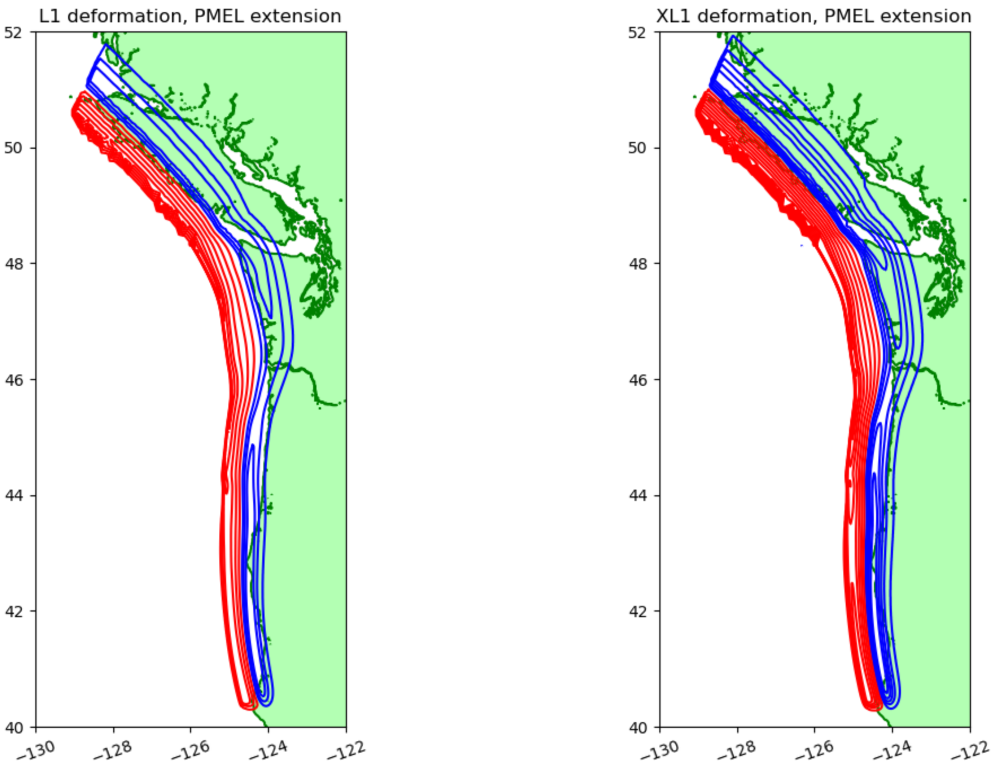

Figure 6: Left: Surface deformation of the L1 source, with maximum uplift 15.08 m and maximum subsidence −3.98 m. Right: Surface deformation of the XL1 source, with maximum uplift 22.62 m and maximum subsidence −5.97 m. In both plots, red contours show uplift (2 meter interval), blue contours show subsidence (1 meter interval).

tried to recreate the deformation field by applying the Okada model to the subfault parameters listed in [6], we determined that the magnitude should be Mw 7.54, as discussed in Appendix E of the Snohomish County report, [16]. Regardless of the proper magnitude, we are using the deformation file provided by PMEL that has been used for the previous tsunami hazard analyses of Everett [6].

Due to uncertainty about the magnitude, in [16] we adopted the SF-L notation for this larger Seattle Fault scenario, and continue to use that here. The deformation was originally chosen to match observed uplift and subsidence at a few points around Puget Sound. Since the original specification of this deformation, many new observations have been made and improved models for the subfault geometry have also been produced. A new model for SF-L is now under development and in the future this could perhaps be used to update the results of the current study.

The Seattle Fault cuts across Puget Sound (through Seattle and Bainbridge Island) and can create a tsunami that affects the southern portion of Whatcom County between 1.5 and 2 hours after the earthquake, and the northern portion after 2 hours. No subsidence or uplift is produced by SF-L in Whatcom County. Tsunami simulations for this source were run out to 8 hours of simulated time. The hypothetical event SF-L considered here does not cause significant inundation or high currents in the `PtRoberts` region, as seen in the figures of Section 6.

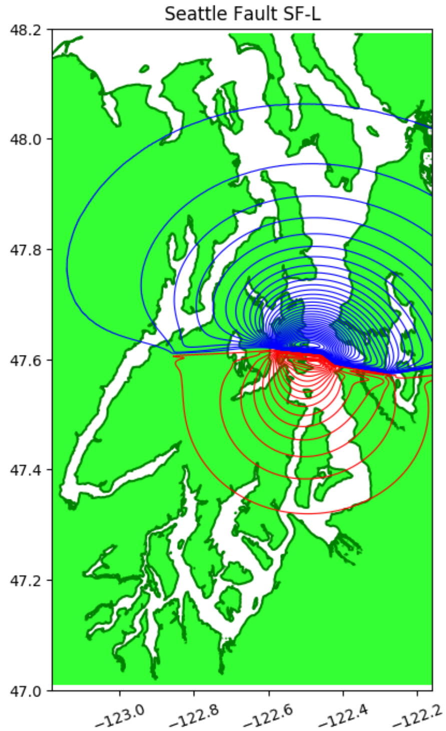

Figure 7: Surface deformation of the SF-L source, with maximum uplift 8.37 m and maximum subsidence −1.78 m. Red contours show uplift, blue contours show subsidence (1 meter intervals in each case).

3.3 Aleutian Subduction Zone event AKmaxWA

The Aleutian Subduction Zone event denoted by AKmaxWA in this study is based on a hypothetical earthquake developed by PMEL in the work reported in [7], shown in Figure 8. This source was designed to have a similar magnitude and location as the 1964 Alaska Earthquake (Mw 9.2) but to have uniform slip of 20 m specified over a set of 20 "unit source" subfaults from the NOAA SIFT database. The set of unit sources used were chosen by running tsunami simulations with all combinations subject to some constraints and choosing the set that gave the maximum impact on the Washington coast. The magnitude based on the subfault dimensions and slip (and assuming a crustal shear modulus, or rigidity, of 40 GPa) works out to Mw 9.24. Since magnitudes are generally rounded off to 1 digit in reporting them, this was viewed as a "maximal Mw 9.2" event, thus having the same magnitude as the 1964 event with maximal impact on Washington.

For more details on this source, including the subfault parameters, and related Alaska sources, see [2].

It takes more than 5 hours for the tsunami to reach the `PtRoberts` study region from the AKmaxWA source region. The maximum depth and flow speed is typically observed between 5 and 12 hours post-earthquake during which time there are 4 waves of similar amplitude. Tsunami simulations for this source were run out to 14 hours of simulated time. Again the gauge results of Section 7 give confidence that this is sufficient to capture the maxima.

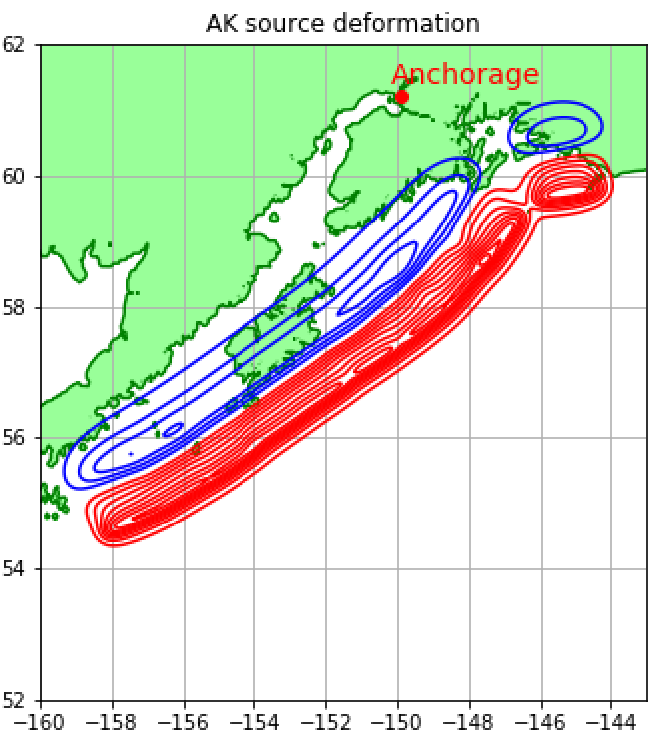

Figure 8: Surface deformation of the AKmaxWA source, with maximum uplift 9.7 m and maximum subsidence −4.9 m. Red contours show uplift, blue contours show subsidence (1 meter intervals in each case).

3.4 Earthquake sources used for Canadian modeling

Recent Canadian modeling [10, 11] has used two CSZ sources and one Alaska source, but they are different from the ones used here. The CSZ sources are from recent work by Gao et al. [12] and are more similar to the M1 source from the work of Witter et al. [31] than to the larger L1 or XL1 sources used here. As a result, our inundation predictions are significantly different from those presented in [10]. The Canadian modeling also used a different Alaska source, a model of the 1964 event from Suleimani [28], as discussed in [11].

4 Modeling uncertainties and limitations

The simulations of tsunami generation, propagation and inundation were conducted with the GeoClaw model. This model solves the nonlinear shallow water equations, has undergone extensive verification and validation (e.g. [5, 19]), and has been accepted as a validated model by the U.S. National Tsunami Hazard Mitigation Program (NTHMP) after conducting multiple benchmark tests as part of an NTHMP benchmarking workshop [14].

Several important geophysical parameters must be set in the GeoClaw software, and some physical processes are not included in these simulations, which use the two-dimensional shallow water equations. These are discussed below along with their potential effect on the modeling results.

4.1 Tide stage and sea level rise

The simulations were conducted with the background sea level set to 0 relative to the DEMs in use, which are referenced to local MHW. This value is conservative, in the sense that the severity of inundation will generally increase with a higher background sea level. Larger tide levels do occasionally occur, but the assumption of MHW is standard practice in studies of this type. Potential sea level rise over the coming decades was not taken into account in this modeling.

The 1/3" DEMs used in this study are all referenced to MHW, meaning that $Z = 0$ corresponds to the shoreline at MHW.

4.2 Subsidence

The CSZ events have significant co-seismic subsidence at all coastal regions in this study. The subsidence is accounted for in the GeoClaw modeling, since the initial DEM provided for the region is modified by the earthquake deformation. The AKmaxWA event produces no deformation in the study region.

4.3 Structures

Buildings were not included in the simulations, the topographic DEMs provided for this study are "bare earth". The presence of structures will alter tsunami flow patterns and generally impede inland flow. To some extent the lack of structures in the model is therefore a conservative feature, in that their inclusion would generally reduce inland penetration of the tsunami wave. However, as in the case of the friction coefficient, impeding the flow can also result in deeper flow in some areas. It can also lead to higher fluid velocities, particularly in regions where the flow is channelized, such as when flowing up streets that are bounded by buildings.

4.4 Bottom friction

Mannings coefficient of friction was set to 0.025, a standard value used in tsunami modeling that corresponds to gravelly earth. This choice of 0.025 is conservative in some sense, because the presence of trees, structures and vegetation would justify the use of a larger value, which might tend to reduce the inland flow. On the other hand, larger friction values can lead to deeper flow in some areas, since the water may pile up more as it advances more slowly across the topography. A sensitivity study using other friction values has not been performed.

4.5 Tsunami modification of bathymetry and topography

Severe scouring and deposition are known to occur during a tsunami, undermining structures and altering the flow pattern of the tsunami itself. Again, this movement of material requires an expenditure of tsunami energy that tends to reduce the inland extent of inundation. On the other hand, if natural berms or ridges along the coastline (or man-made levies or dikes) are eroded by the tsunami, then some areas can experience much more extensive flooding. There is no erosion or deposition included in the simulations presented here.

5 Study regions

Figure 1 shows the portion of the coast considered, the two yellow polygons covering the study region. These regions will be referred to as *fgmax regions* since these are regions on which a fixed set of points is defined (independent of adaptive refinement) on which the maximum of each quantity of interest is monitored during the course of the simulation. The quantities monitored are the flow depth, flow speed, and momentum flux, along with the time at which the maximum is attained and the first arrival time of significant waves at each grid point.

Within each fgmax region, a set of fgmax points were defined as described below, the points where the maxima need to be monitored. For each tsunami source, a separate job run was then done for each region in which adaptive mesh refinement (AMR) was used to focus fine computational grids around the fgmax region. Due to the large extent of the study region and complicated coastline, it was not possible to do a single run with 1/3" resolution around all the fgmax regions. Table 1 gives an overview of the two regions.

Region label	Count	Plots and Results
`PtRoberts`	2,271,534	Section 6.1
`Semiahmoo`	1,477,749	Section 6.2
Total	3,749,283	

Table 1: The fgmax regions. The fgmax points are aligned with the DEM in the regions specified, with 1/3" spacing in longitude and latitude. The column labeled "Count" gives the number of fgmax points in each region. The colored points in Figure 2 are all the fgmax points from both study regions. See Figure 3 and Figure 4 for plots of the fgmax points in regions `PtRoberts` and `Semiahmoo`, respectively, and Section 6 for plots of some sample results for each region.

The fgmax points lie on a grid with spacing 1/3" by 1/3" that is aligned with the DEM grids. We select only the points from the 1/3" grid that satisfy all of these conditions:

- The point lies within a specified polygon,
- The point has a topography elevation below a specified maximum $Z_{\max}$,
- There is a path of points with elevation below $Z_{\max}$ connecting the point to the coast.

In addition, any grid point in the polygon that lies within 20 grid cells of the coast is selected as an fgmax point, insuring that there is a band of fgmax points all along the coast, even in regions where the topography rises very steeply. This approach is discussed in more detail in [2]. For this project we chose $Z_{\max} = 15$ m, based on some initial simulations that showed that the sources we considered did not runup values exceeding this value in the study regions.

If only onshore inundation and near shore currents need to be modeled, then one could also set a lower threshold, e.g. -60 m, and only select fgmax points within the polygons where the bathymetry elevation is both above this value and less than $Z_{\max}$. For this project we included all water points in each polygon in order to model currents farther from shore.

6 Results – Maximum flow depth and speeds

We have not attempted to produce high quality graphics of the results, since the Washington Geological Survey (WGS) is producing the maps that will be published elsewhere. However, in Figures 9–11 we provide some plots to give an indication of the sort of flooding and flow speeds observed, and for future reference if the simulations are re-run at a later date.

The maximum flow depth plots show the maximum depth of water recorded during the computation over the full simulation time of 10 hours for the CSZ events, 8 hours for SF-L, and 14 hours for theAKmaxWA. This depth is shown only in regions that were originally dry in the simulation, and those points colored green remained dry. White regions are where there was initially water, or else there were no fgmax points. In the speed plots the maximum speed is shown both in the water and for initially dry points that became wet at some point. White regions are where there were no fgmax points.

In addition to the plots shown in this report, we have also produced high-resolution png files in a form that has been embedded in kml files to facilitate viewing the input data and results on Google Earth, for example. The low resolution figures in this report cannot possibly show all the details whereas with the kml files the user can zoom in to explore the results in more detail.

These kml files can be found at [18], along with the Python code that produced them.

The raw results are contained in netCDF files posted at [18], and these can be downloaded and plotted in different ways or with different color maps, either using modifications of our Python scripts, or with sophisticated GIS tools.

For each region we point out some noteworthy aspects of the simulation results in the pages below. We give an indication of the arrival time of each tsunami in each region, as determined by inspection of the gauges at interfaces between the different fgmax regions; see Section 7.

6.1 Region `PtRoberts`

Figure 3 shows the topography of the fgmax points selected in the `PtRoberts` region. Figure 9 and Figure 10 show some sample results for this region.

Noteworthy in this region.

- The arrival of the first positive wave (5 cm above MHW) is at 2 hours, 11 minutes postquake for the CSZ-L1 and CSZ-XL1 events, 1 hour and 54 minutes for SF-L and 5 hours and 10 minutes for AKmaxWA in the offshore region around Point Roberts near gauge 303. Similar arrival times were seen for the first positive wave (5cm above MHW) for gauges 300, 302, and 305.
- The wave amplitudes were higher with CSZ-L1 and CSZ-XL1 than with the far field AKmaxWA source. For example, at Gauge 303 at Point Roberts Lily Point, the maximum CSZ-XL1 amplitude was around 2.5m, the maximum CSZ-L1 amplitude around 1.5m, while that of the AKmaxWA source had 4 waves with amplitudes around 0.5m.
- The AKmaxWA source produced multiple waves of around the same amplitude between 5.5 to 13 hours post-quake at Gauge 303. The largest amplitude at Gauge 303 for the CSZ sources was the first wave, but two additional waves with amplitudes above 1m (for CSZ-XL1) and 0.5m (for CSZ-L1) were observed up through 7 hours post-quake, and waves with diminishing amplitude continued throughout the 14 hour simulation.
- The speeds were higher with CSZ-L1 and CSZ-XL1 than with the far field AKmaxWA source. For example, at Gauge 303 at Point Roberts Lily Point, the maximum CSZ-XL1 speed was around 2.5m/sec,

the maximum CSZ-L1 speed was between 1.75m/sec and 2.0 m/sec, while that of the AKmaxWA source was less than 1.4m/sec.

- Point Roberts Marina sees wave amplitudes between 1.5 and 2.0 meters with CSZ-XL1, between 1.0 and 1.5 meters with CSZ-L1, and between 0.5 and 1.0 meters with AKmaxWA.
- Boundary Bay sees wave amplitudes between 2.0 and 4.0 meters with CSZ-XL1, between 1.5 and 4.0 meters with CSZ-L1, and between 1.0 and 1.5 meters with AKmaxWA. In the waters near the southern and western coasts of Point Roberts, wave amplitudes were between 1.5 and 2.0 meters for CSZ-XL1, between 1.0 and 1.5 meters for CSZ-L1, and between 0.5 and 1.0 meter for AKmaxWA.
- The largest speeds offshore were seen off Lily Point for the CSZ-XL1, CSZ-L1, and AKmaxWA sources.
- The SF-L source produces very little inundation and speeds in the PtRoberts region. For example, the maximum wave amplitude seen at the gauges 300, 302, 303, and 305 around Point Roberts was less than 0.1 meters and the maximum speed did not exceed 0.175 m/sec.
- No inundation was seen at Gauge 304 from any of the sources. This gauge was located onshore in west Point Roberts. Point Roberts Airpark and Point Roberts Marina Resort also stay dry with all the sources.
- The maximum onshore inundation and speeds in this region were seen along the eastern coast of Tsawwassen in and around Boundary Bay Regional Park in Canada. Note that much of this region is below MHW (see Figure 3).
- This region experiences no subsidence or uplift with any of the sources considered.

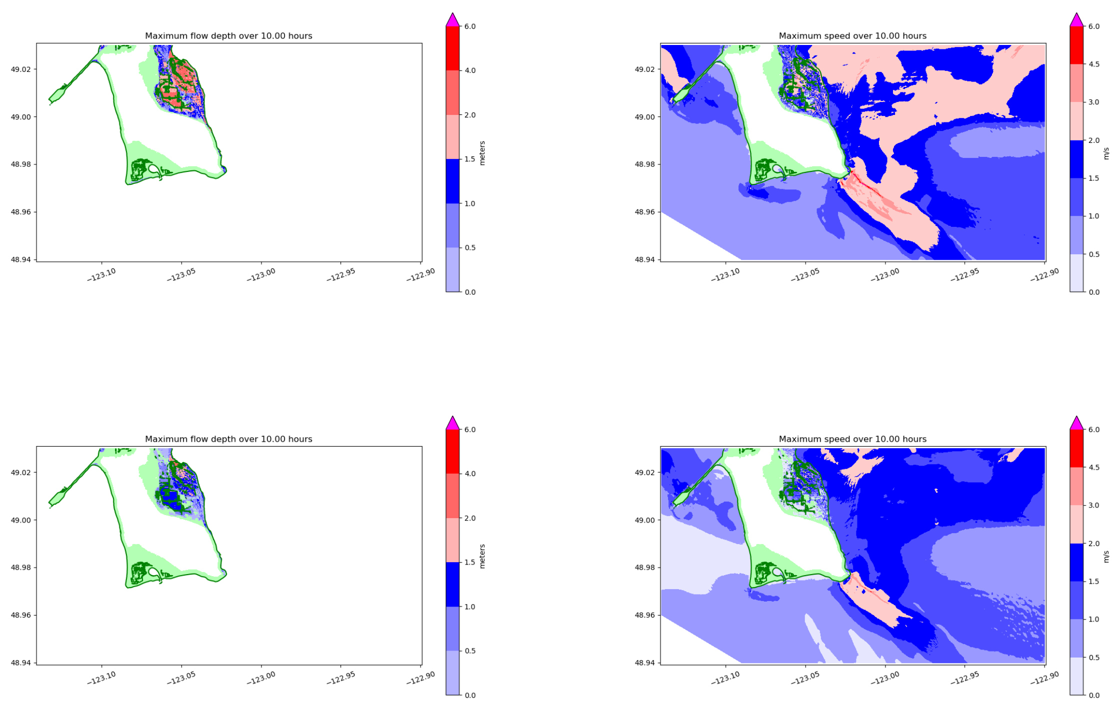

Figure 9: Sample results for the Region `PtRoberts`. See the description in Section 6.1. Top: CSZ-XL1, Bottom: CSZ-L1. Plots on the left show maximum flooding depth (m) for initially-onshore points, those on the right show maximum flow speed (m/s) for all fgmax points. The fgmax points colored green remained dry in the simulation.

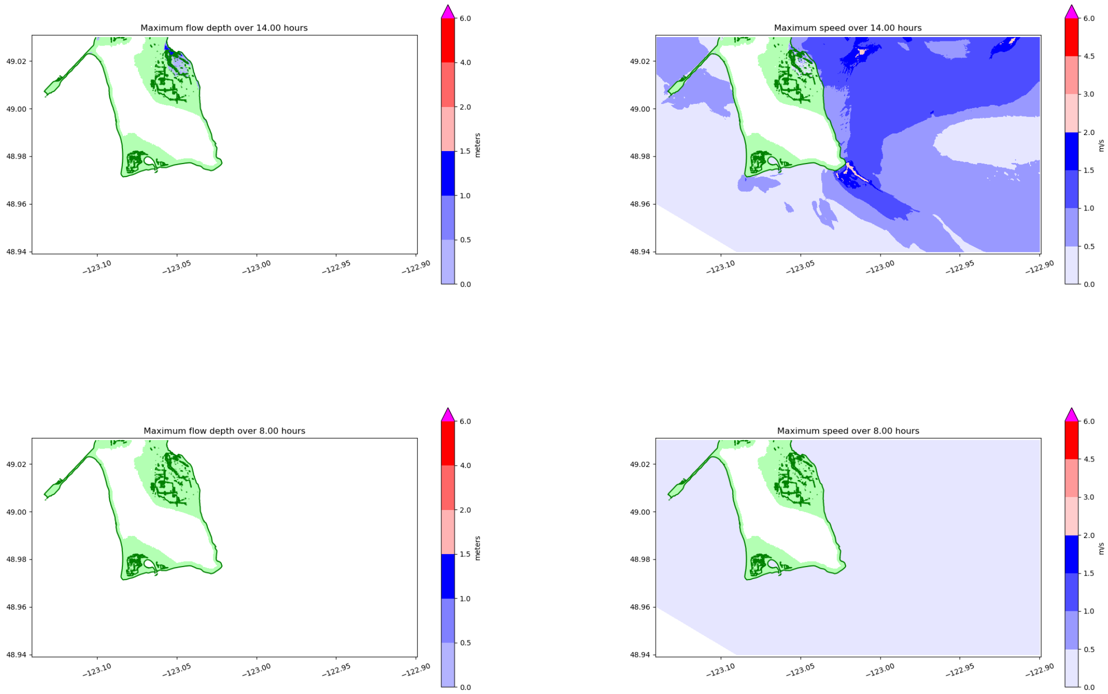

Figure 10: Sample results for the Region `PtRoberts`. See the description in Section 6.1. Top: AKmaxWA, Bottom: SF-L. Plots on the left show maximum flooding depth (m) for initially-onshore points, those on the right show maximum flow speed (m/s) for all fgmax points. The fgmax points colored green remained dry in the simulation.

6.2 Region `Semiahmoo`

Figure 4 shows the topography of the fgmax points selected in the `Semiahmoo` region. Figure 11 shows some sample results for this region.

Noteworthy in this region.

- Only the CSZ-L1 source was considered in this region.
- Gauges 301 and 361 in Drayton Harbor correspond to gauges 1 and 61 from the 2018 Whatcom County modeling [1]. Comparisons of these gauges are provided in Appendix C.
- The arrival of the first positive wave (5 cm above MHW) was 2 hours and 14 minutes post quake at the approach to Drayton Harbor as recorded by gauge 301.
- The first wave was the highest with amplitude 2.5 meters, but two additional waves with amplitudes 1.95 and 1.26 meters were observed up through 7 hours post-quake, and waves with diminishing amplitude continued throughout the 10 hour simulation.
- Speeds just over 5 meters/sec were seen at gauge 301 for this CSZ-L1 event.
- Semiahmoo Bay sees amplitudes between 2 and 4 meters and Drayton Harbor between 1.5 and 2 meters.
- The US Border Patrol at Blaine stays dry, but 1 to 2 meters of flooding from the east end of Drayton Harbor continues up a river that is crossed by Peace Portal Drive and 1.5 meters continues to cross (or go under) I-5. In addition, there might be an active railway paralleling Peace Portal Drive that could be impacted.
- Blaine Animal Hospital and Semiahmoo Resort Golf Spa stay dry, but Semiahmoo Resort Association sees up to 0.5 meters of flooding.
- Onshore flooding occurs along Marine Drive in Blaine Harbor, along Semiahmoo Parkway and Drayton Harbor Road and up two river valleys (separated by I-5) at the east end of Drayton Harbor.
- This region experiences no subsidence or uplift with any of the sources considered.

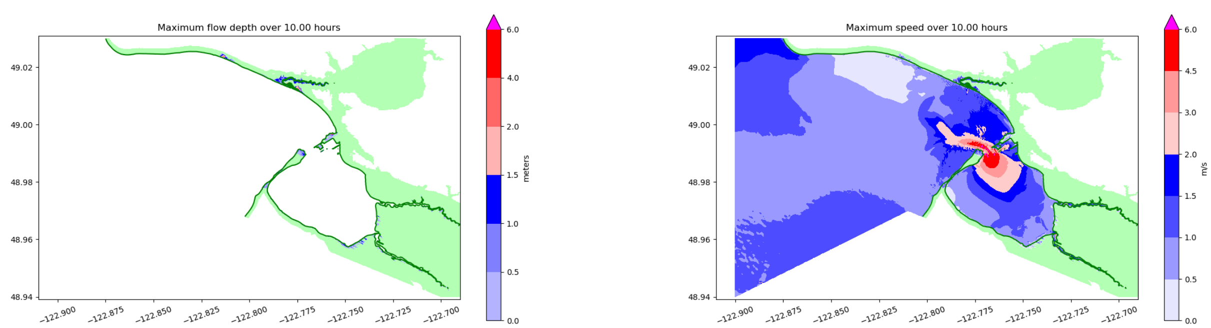

Figure 11: Sample CSZ-L1 results for the Region `Semiahmoo`. See the description in Section 6.2. Plots on the left show maximum flooding depth (m) for initially-onshore points, those on the right show maximum flow speed (m/s) for all fgmax points. The fgmax points colored green remained dry in the simulation.

7 Results – Gauge output

Table 2 and Figures 12 and 13 show the location of the simulated gauges used to capture time series of the flow depth / surface elevation and of the current velocity over the course of each simulation, as specified by WGS and summarized in Tables 2. All of the gauges fall within the 1/3" by 1/3" *fgmax regions* listed in Table 1, and the time series for these were calculated from the run in the fgmax region containing the gauge.

No.	Longitude	Latitude	Location	Region
300	-123.05325580	48.97281405	Point Roberts	PR
302	-123.06350000	48.97590000	Point Roberts Marina Entrance	PR
303	-123.02000000	48.97800000	Point Roberts Lily Point	PR
304	-123.08200000	48.98250000	Onshore West Point Roberts	PR
305	-123.08700000	48.98250000	Offshore West Point Roberts	PR
310	-123.13310000	49.00560000	Tsawwassen Ferry	PR
311	-123.11640000	49.01610000	Tsawwassen Ferry Pier	PR
312	-123.04860000	49.01320000	Boundary Bay Regional Park	PR
320	-123.05460000	49.02900000	East shore of Tsawwassen	PR
301	-122.76937670	48.99208359	Drayton Harbor approach	SE
361	-122.76000000	48.98000000	Drayton Harbor	SE

Table 2: Location of synthetic gauges, see also the maps in Figures 12 and 13. For each gauge we indicate in column "Region" which of the runs is used to compute the gauge output. The notation PR, and SE are used in this column to denote `PtRoberts`, and `Semiahmoo`, respectively.

In the `Semiahmoo` region we only show two gauges 301 and 361 in Drayton Harbor, which correpond to gauges 1 and 61 respectively from the 2018 Whatcom County report [1]. Comparisons of the new results with the previous results at these gauges are provided in Appendix C.

The figures starting on page 22 show time series output for the synthetic gauges in the `PtRoberts` region. For each gauge, the figures show the surface elevation and speed, for each of the four events. The speed is shown both as a time series of speed $\sqrt{u^2+v^2}$ vs. time, and also in the u–v plane as the red curve in the lower right plot for each event. This plot allows one to see how the E–W component u of the speed compares to the N–S component v, and for some gauge locations shows a strong dominant direction of the current. At other gauges the speed is less strongly one-dimensional.

Note that the vertical scale for each surface elevation and speed plot varies between locations and events in order to clearly show the results, and is set by the maximum amplitude in each case. Note that the CSZ-XL1 seafloor deformation is simply a magnified version of the CSZ-L1 deformation and so the wave patterns for these two events are very similar, but with different magnitudes. Onshore inundation patterns may be very different, however, and this also induces nonlinear differences in reflected waves at offshore gauges.

Examining these gauges gives an indication that the run times chosen for these simulations were sufficiently long to capture the maximum depth and speed at each point.

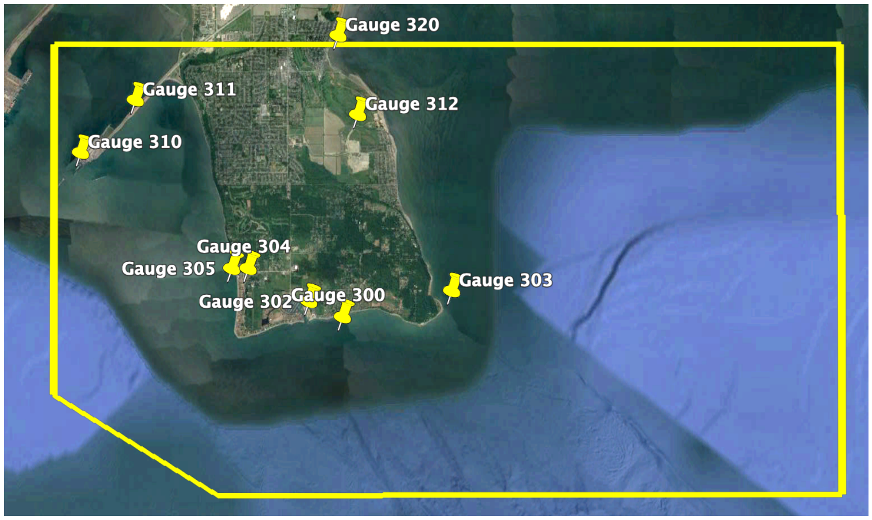

Figure 12: Synthetic gauge locations used in the `PtRoberts` fgmax region. Imagery from Google Earth.

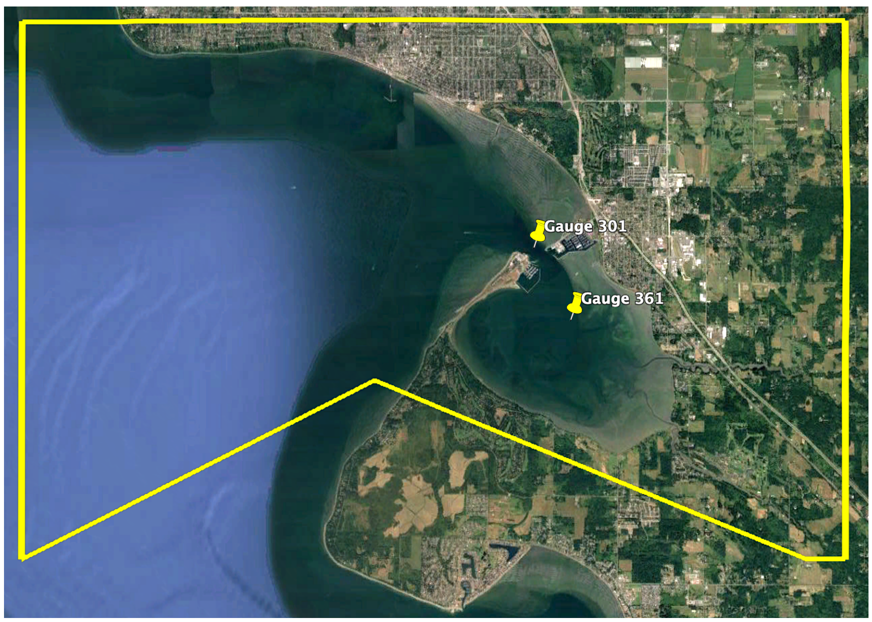

Figure 13: Synthetic gauge locations used in the `Semiahmoo` fgmax region. Imagery from Google Earth.

Gauge 300: Point Roberts

Computed on region `PtRoberts`.

CSZ XL1 event:

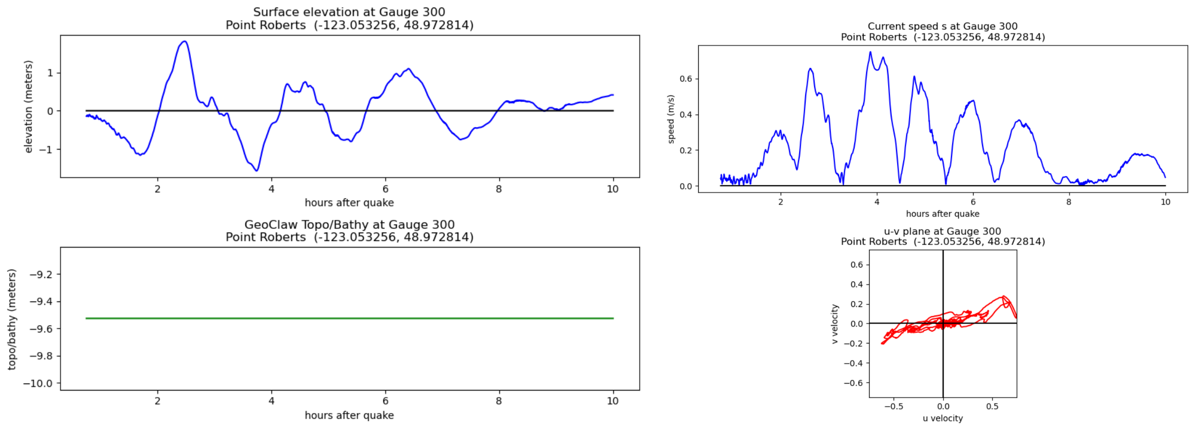

CSZ L1 event:

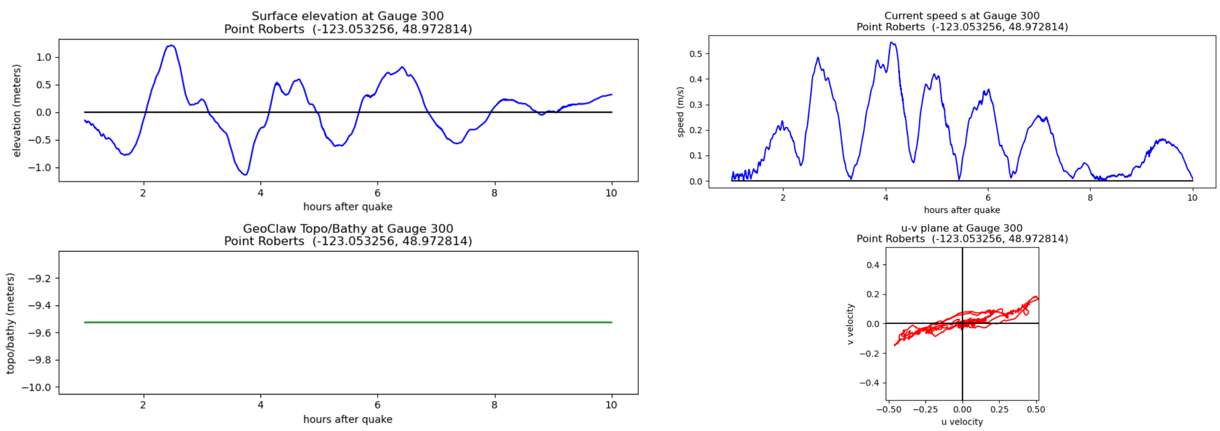

Gauge 300: Point Roberts

Computed on region `PtRoberts`.

AKmaxWA event:

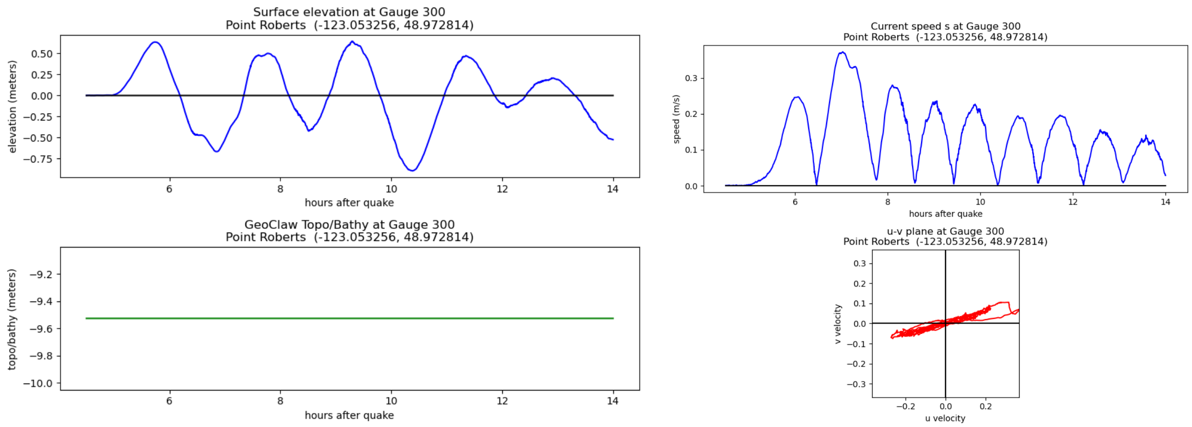

SFL event:

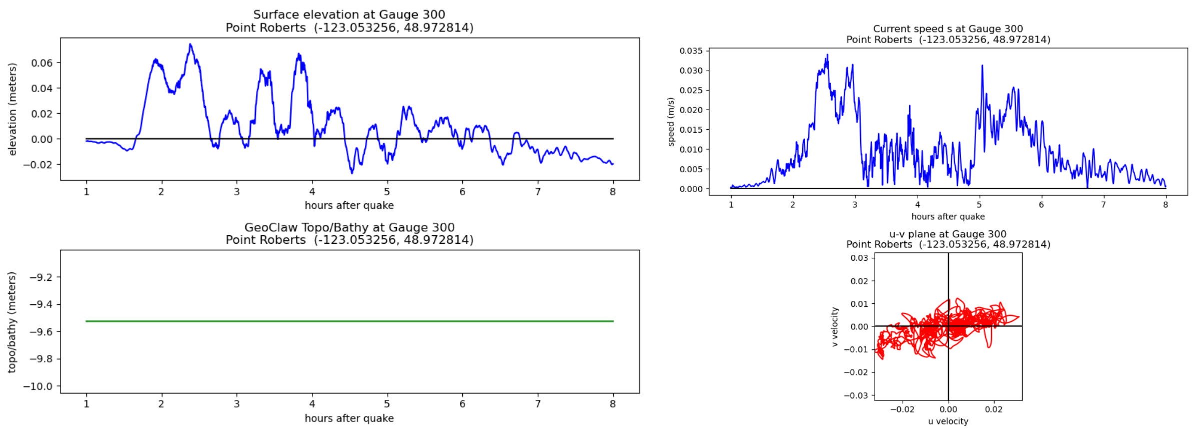

Gauge 302: Point Roberts Marina Entrance

Computed on region `PtRoberts`.

CSZ XL1 event:

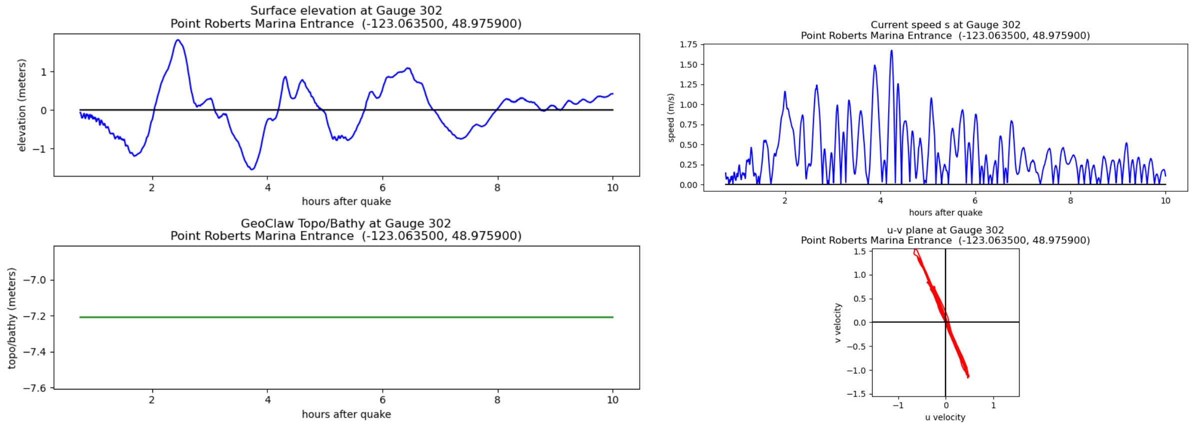

CSZ L1 event:

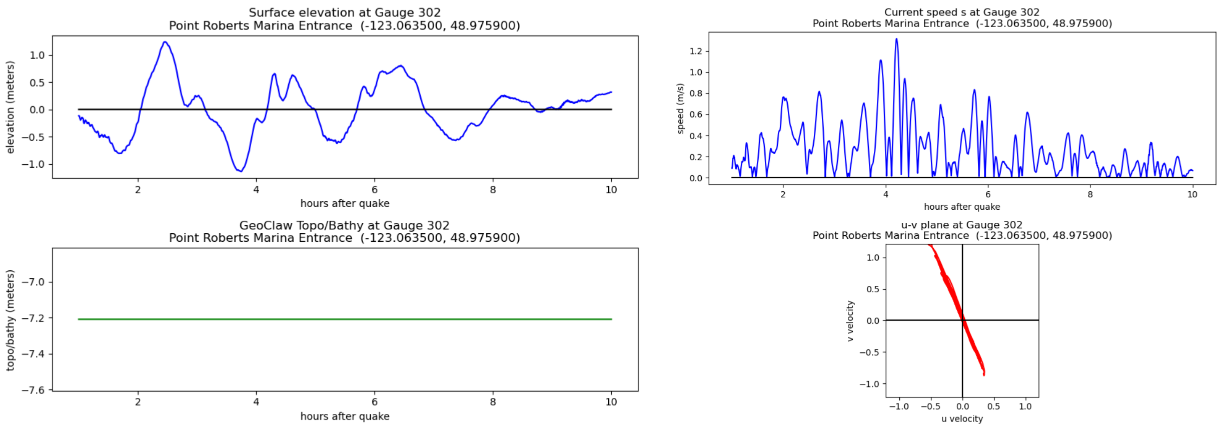

Gauge 302: Point Roberts Marina Entrance

Computed on region `PtRoberts`.

AKmaxWA event:

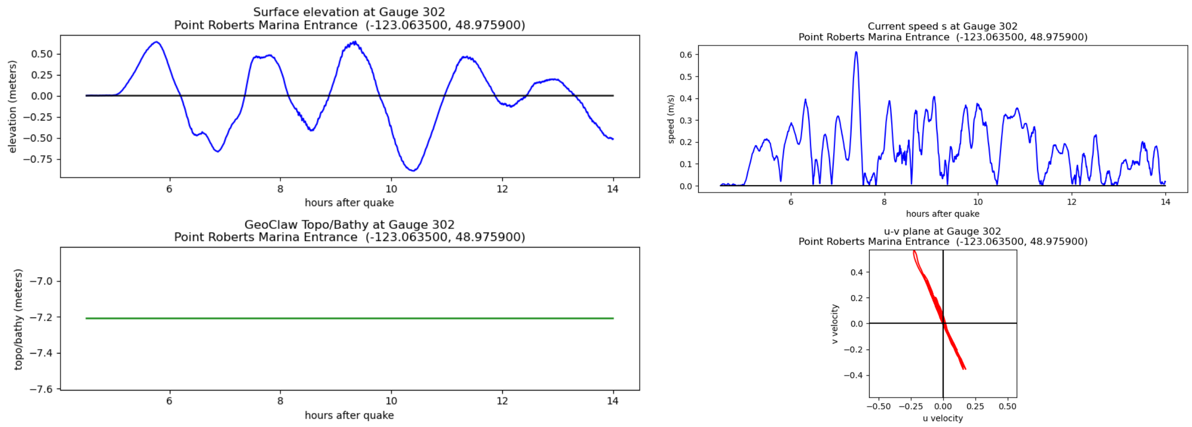

SFL event:

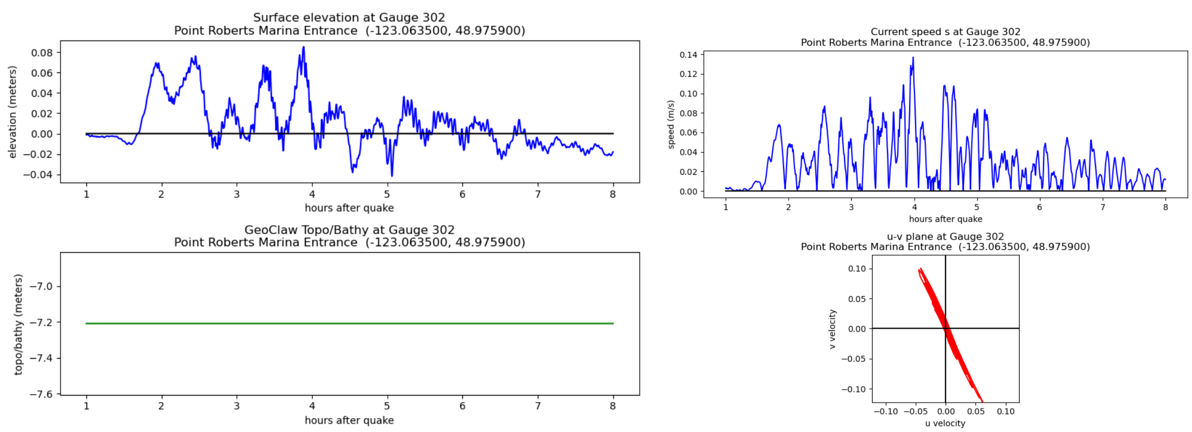

Gauge 303: Point Roberts Lily Point

Computed on region `PtRoberts`.

CSZ XL1 event:

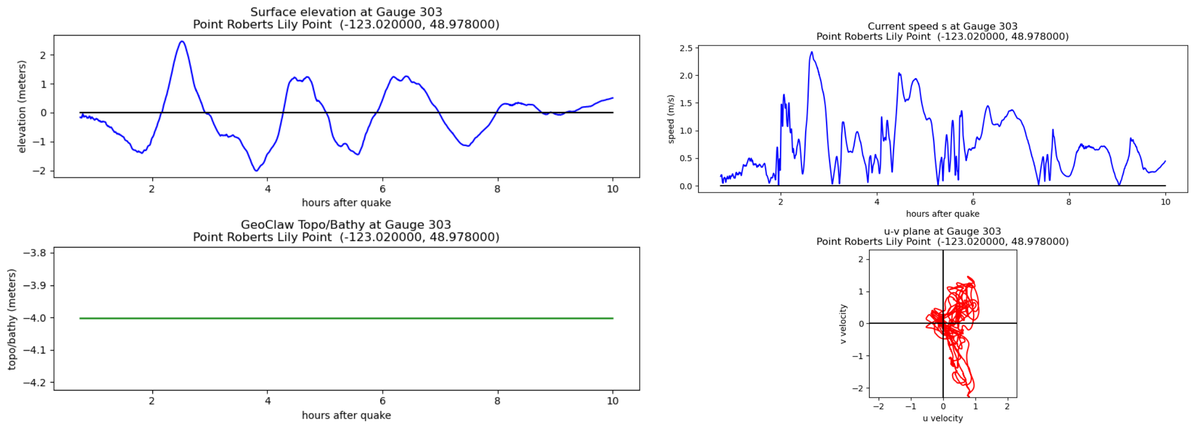

CSZ L1 event:

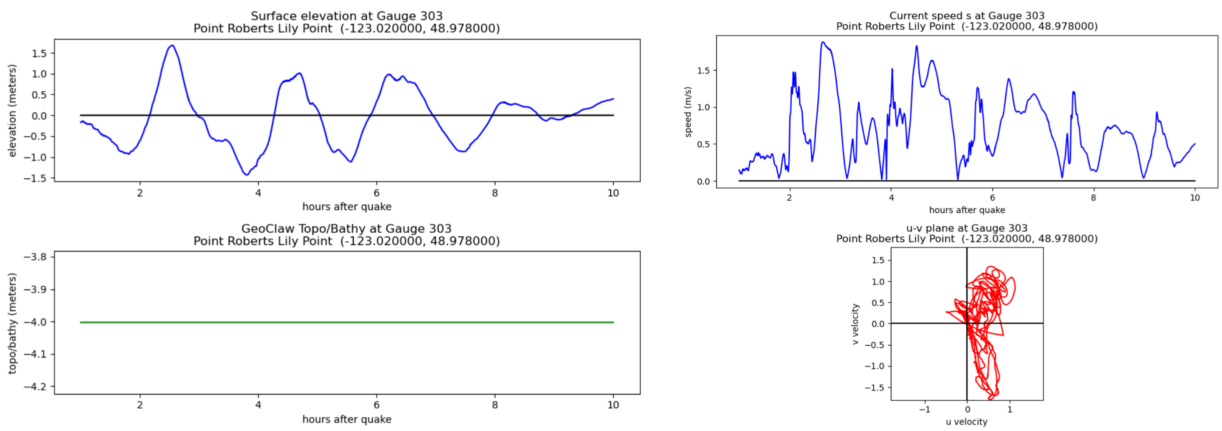

Gauge 303: Point Roberts Lily Point

Computed on region `PtRoberts`.

AKmaxWA event:

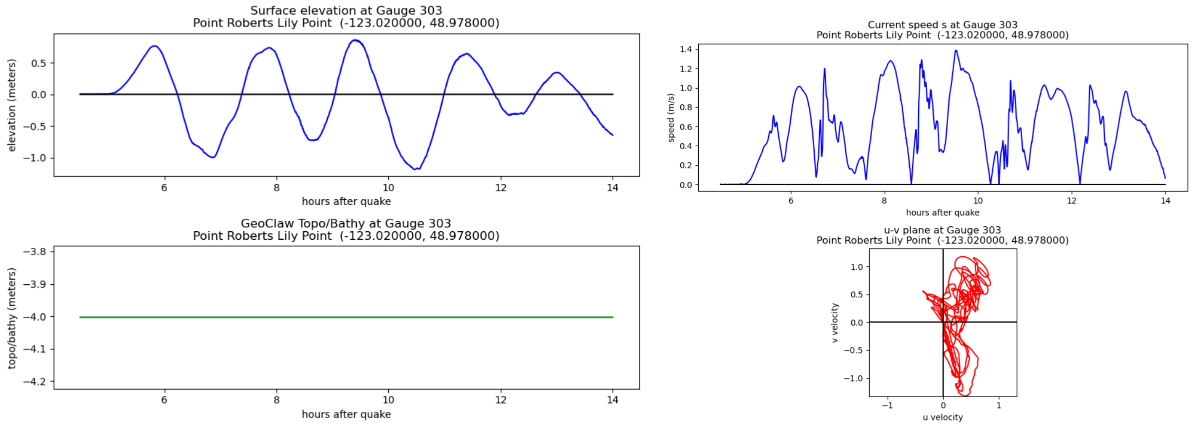

SFL event:

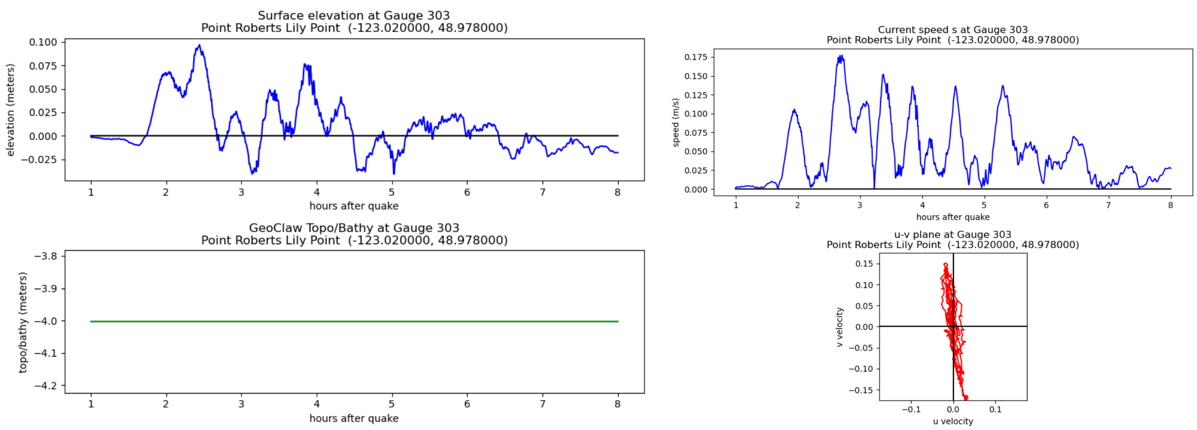

Gauge 304: Onshore West Point Roberts

Computed on region `PtRoberts`.

CSZ XL1 event:

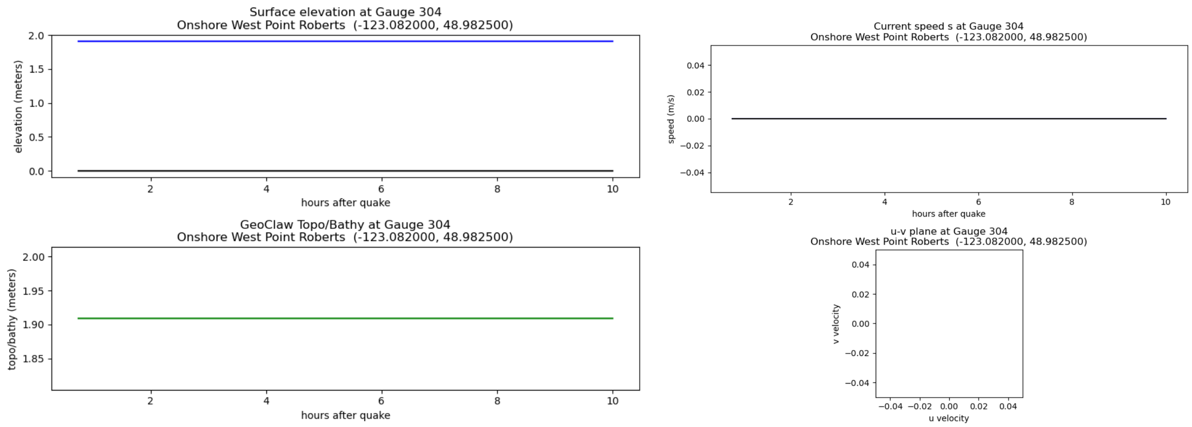

CSZ L1 event:

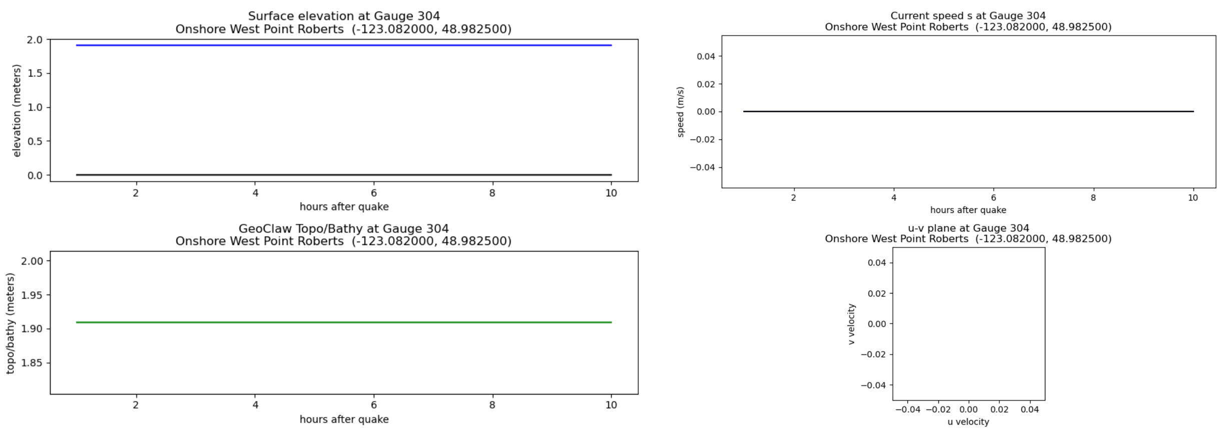

Gauge 304: Onshore West Point Roberts

Computed on region `PtRoberts`.

AKmaxWA event:

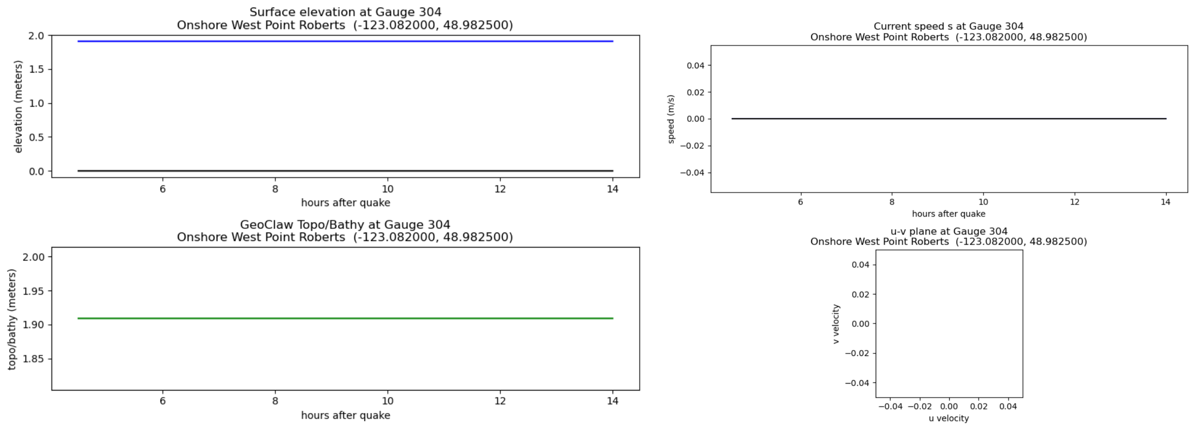

SFL event:

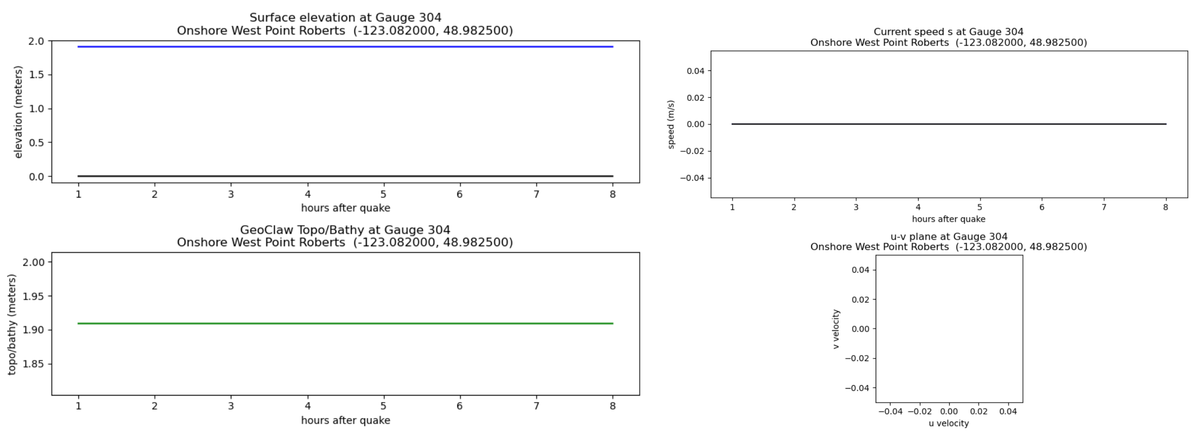

Gauge 305: Offshore West Point Roberts

Computed on region `PtRoberts`.

CSZ XL1 event:

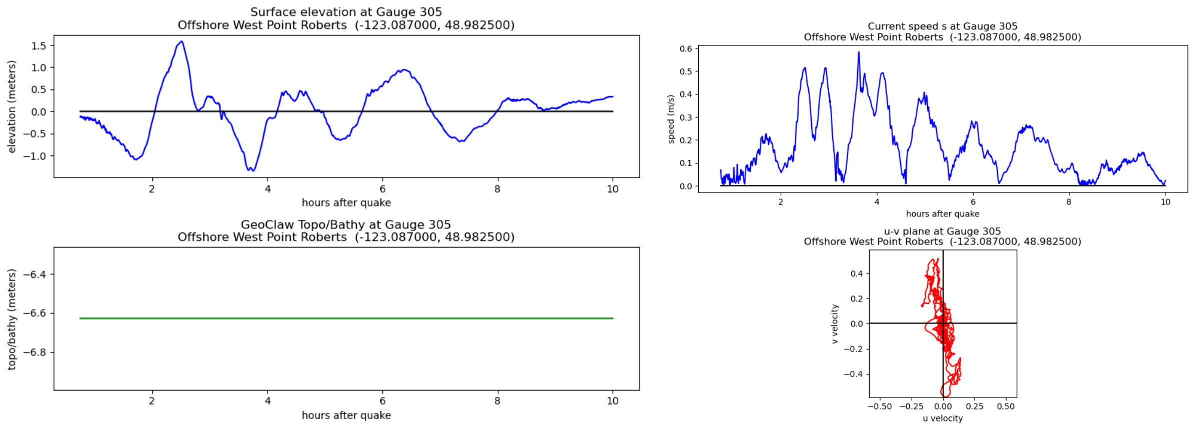

CSZ L1 event:

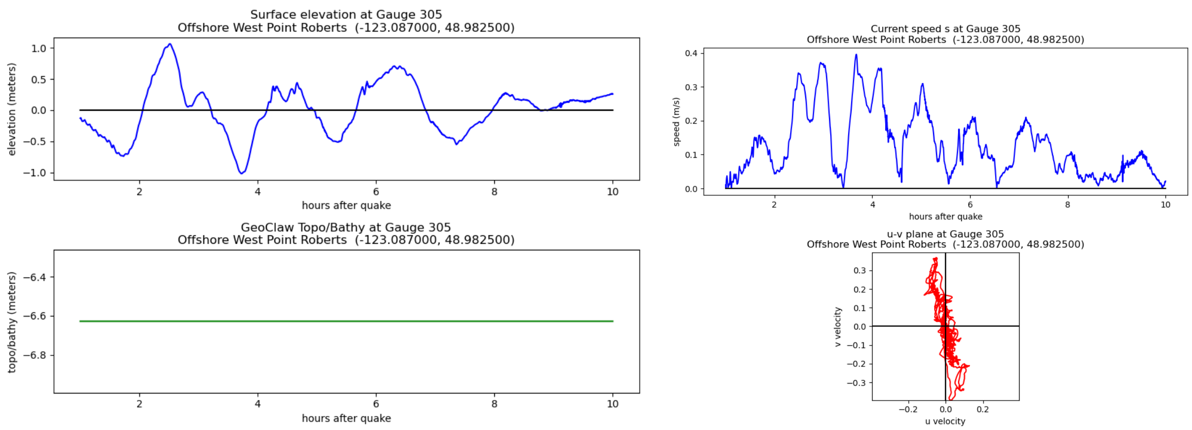

Gauge 305: Offshore West Point Roberts

Computed on region `PtRoberts`.

AKmaxWA event:

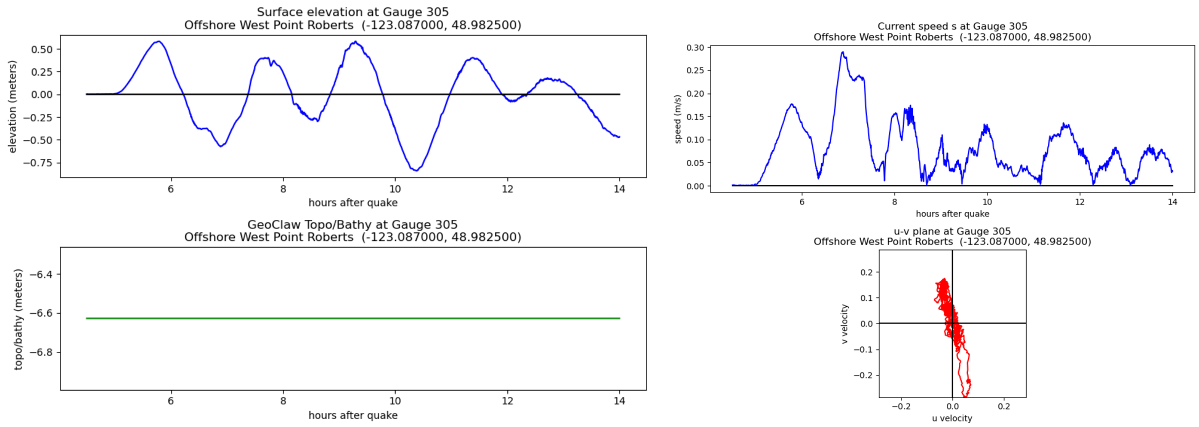

SFL event:

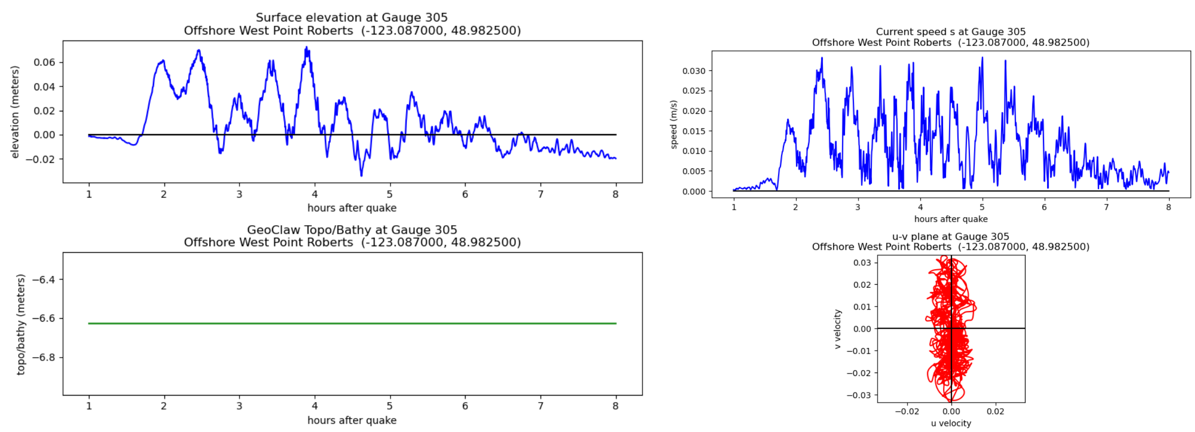

Gauge 310: Tsawwassen Ferry

Computed on region `PtRoberts`.

CSZ XL1 event:

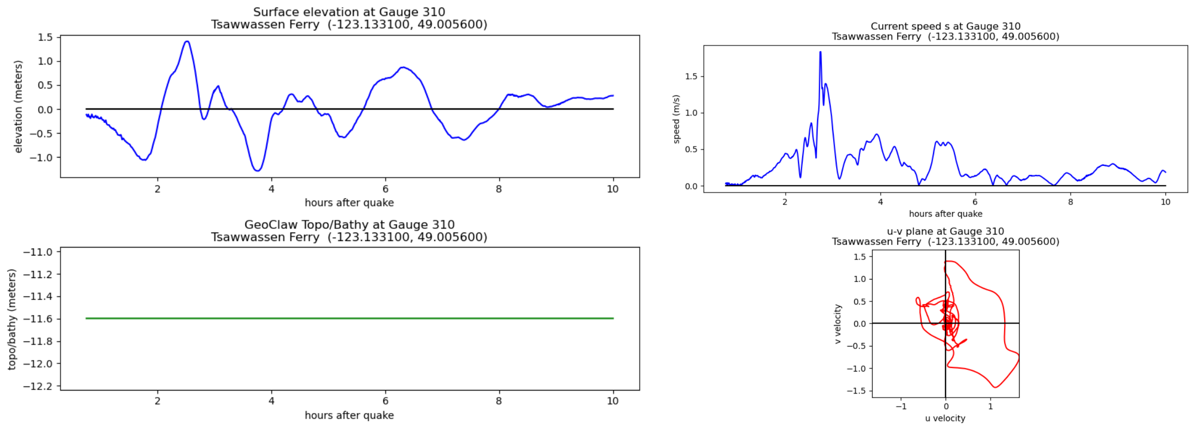

CSZ L1 event:

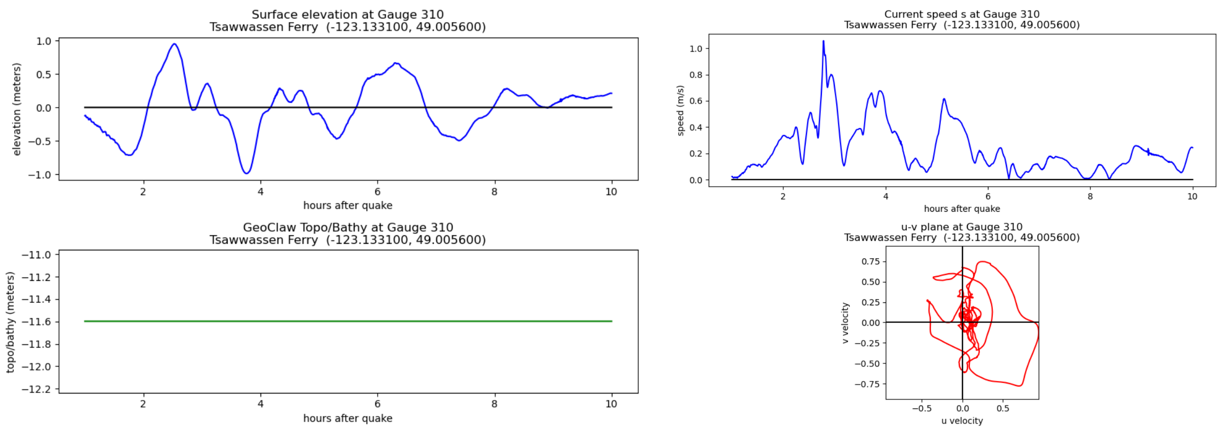

Gauge 310: Tsawwassen Ferry

Computed on region `PtRoberts`.

AKmaxWA event:

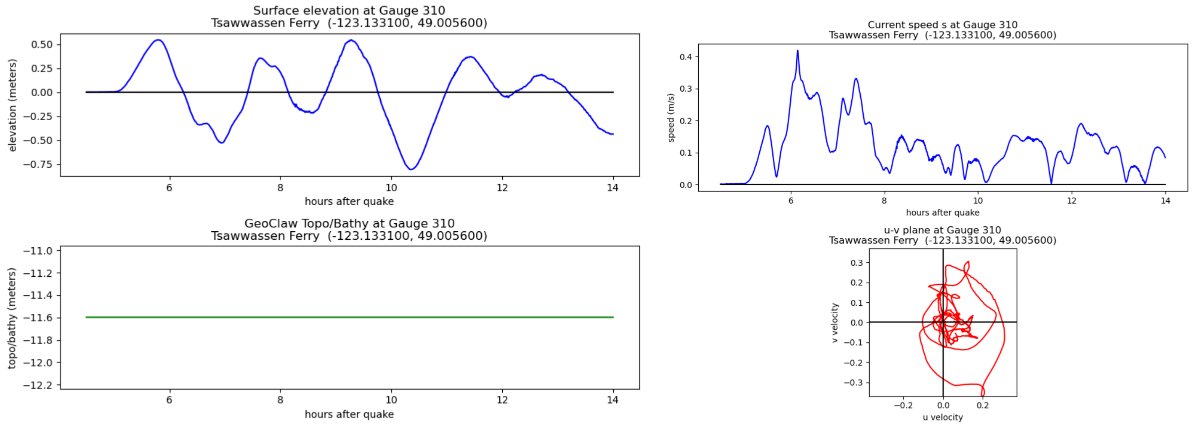

SFL event:

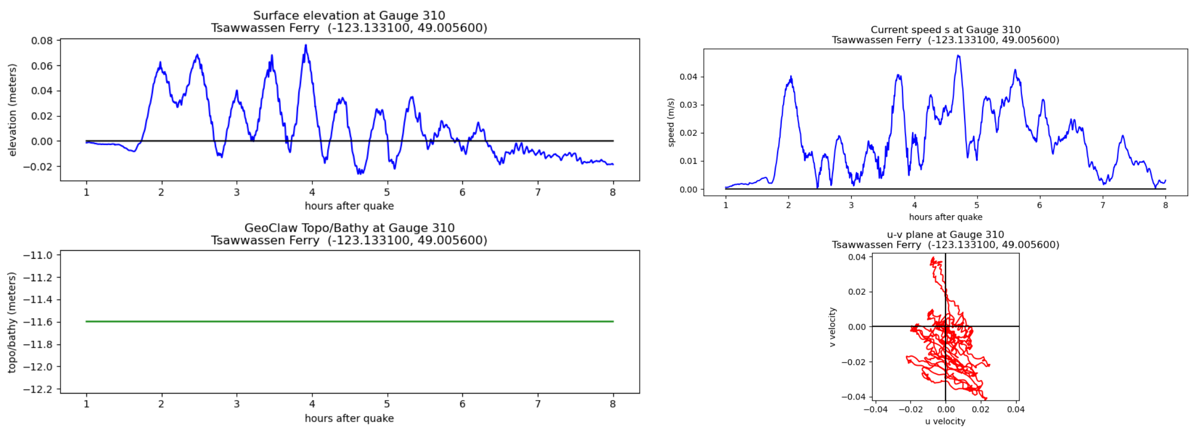

Gauge 311: Tsawwassen Ferry Pier

Computed on region `PtRoberts`.

CSZ XL1 event:

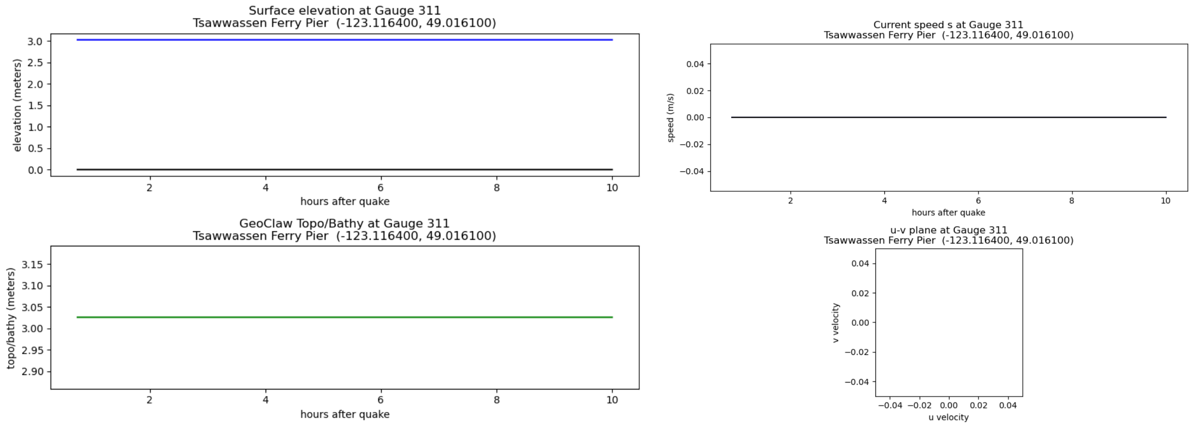

CSZ L1 event:

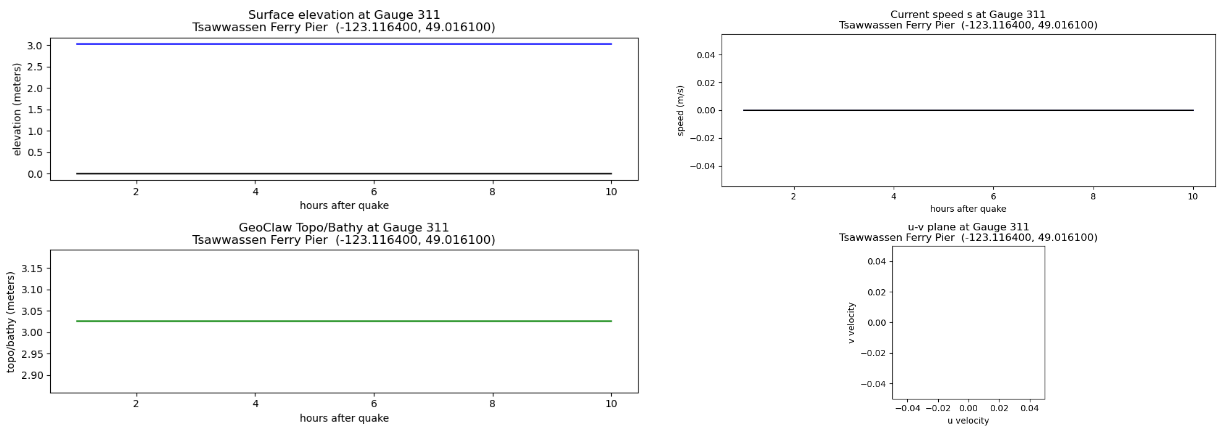

Gauge 311: Tsawwassen Ferry Pier

Computed on region `PtRoberts`.

AKmaxWA event:

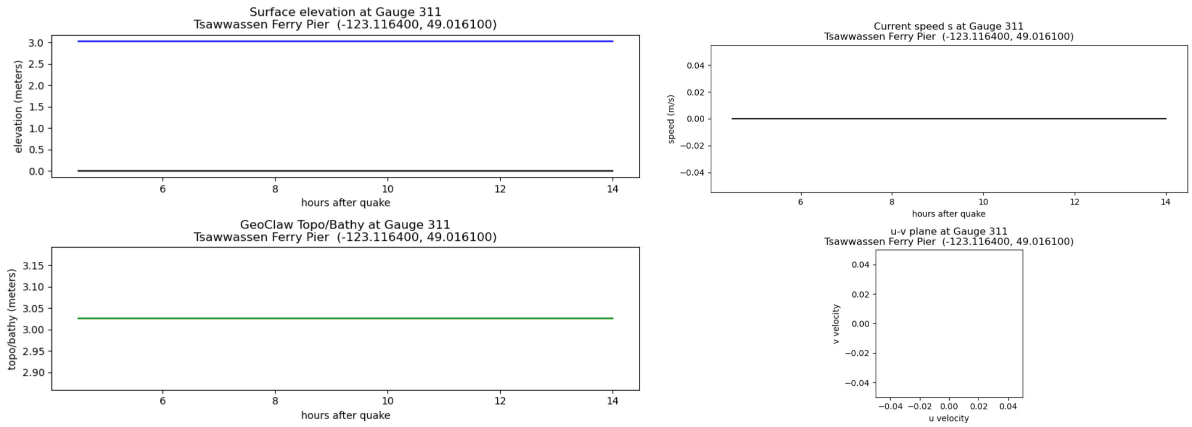

SFL event:

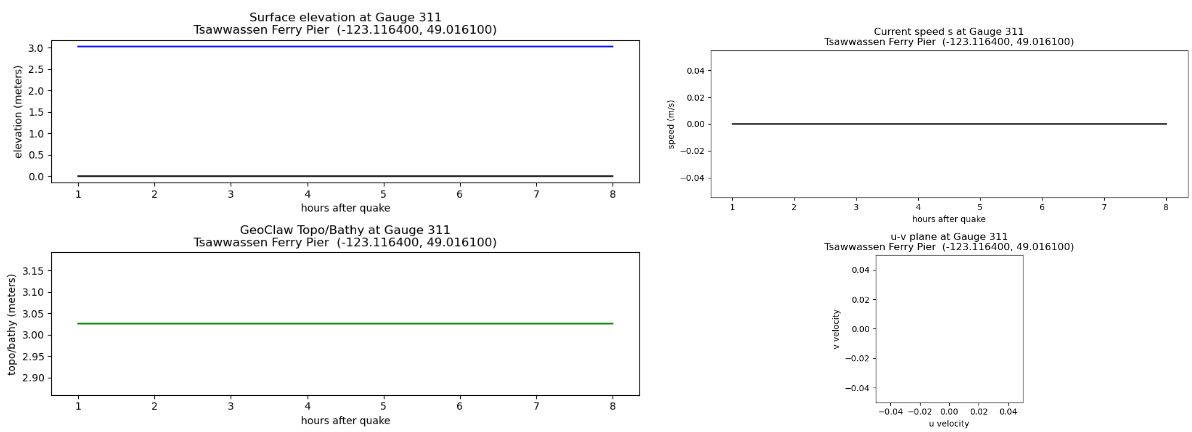

Gauge 312: Boundary Bay Regional Park

Computed on region `PtRoberts`.

CSZ XL1 event:

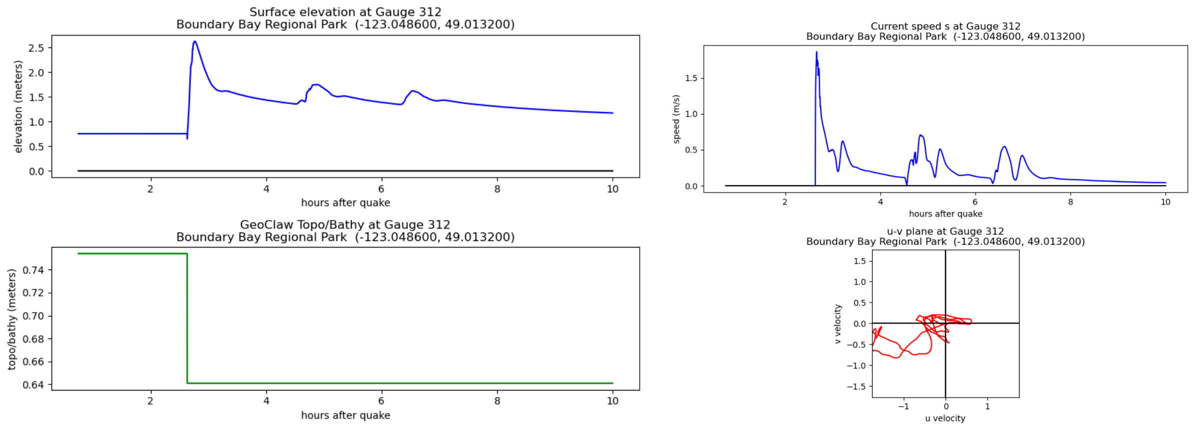

CSZ L1 event:

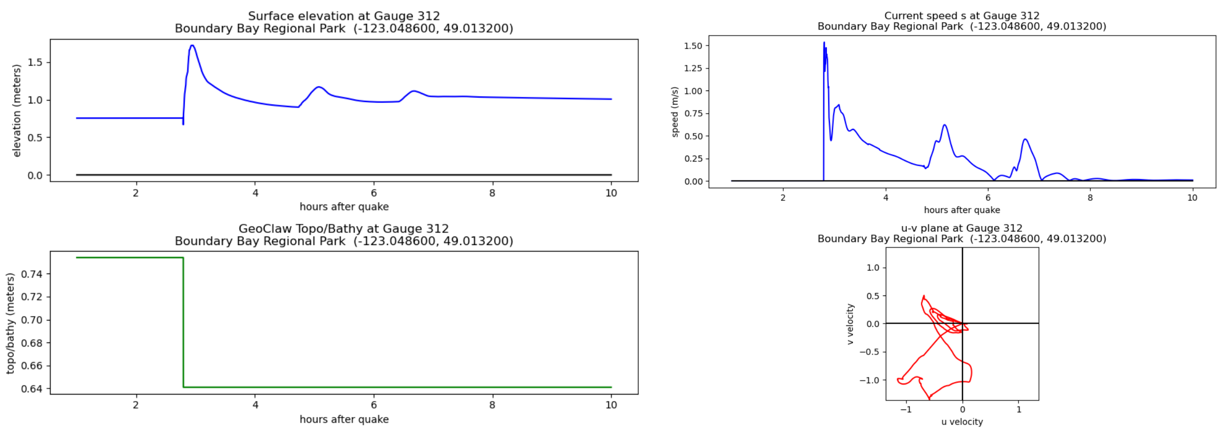

Gauge 312: Boundary Bay Regional Park

Computed on region `PtRoberts`.

AKmaxWA event:

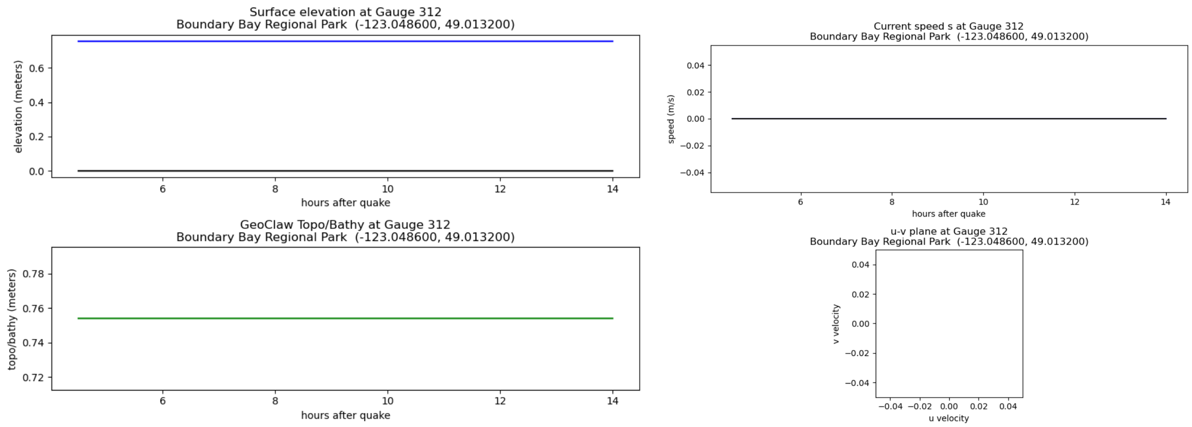

SFL event:

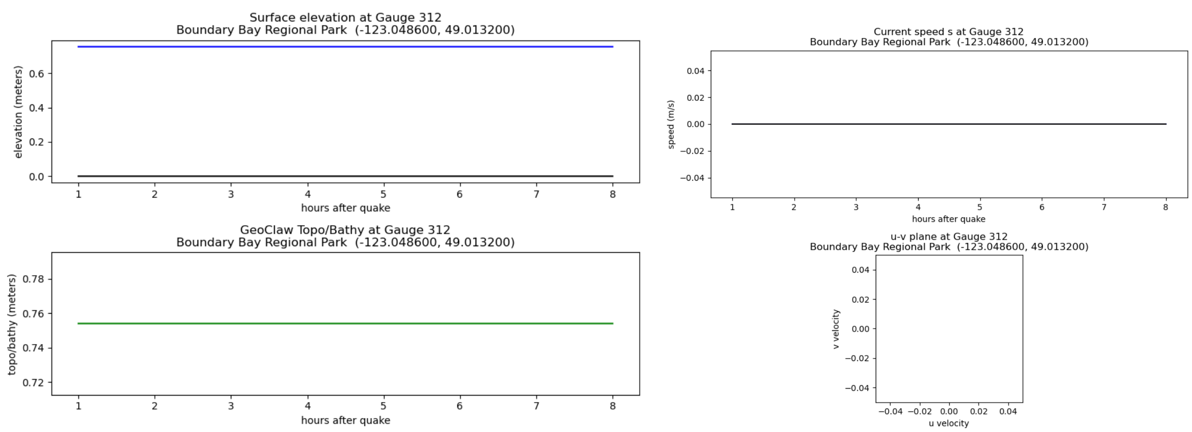

Gauge 320: East shore of Tsawwassen

Computed on region `PtRoberts`.

CSZ XL1 event:

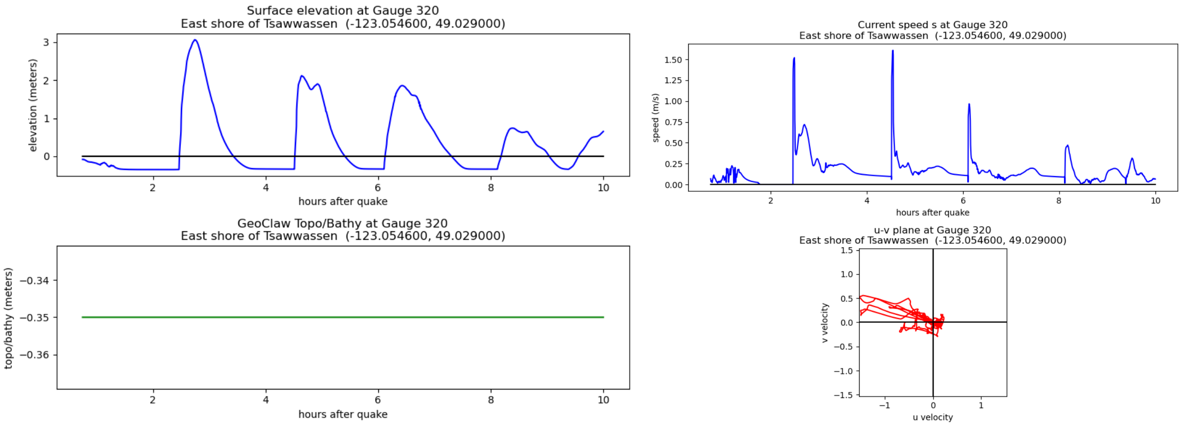

CSZ L1 event:

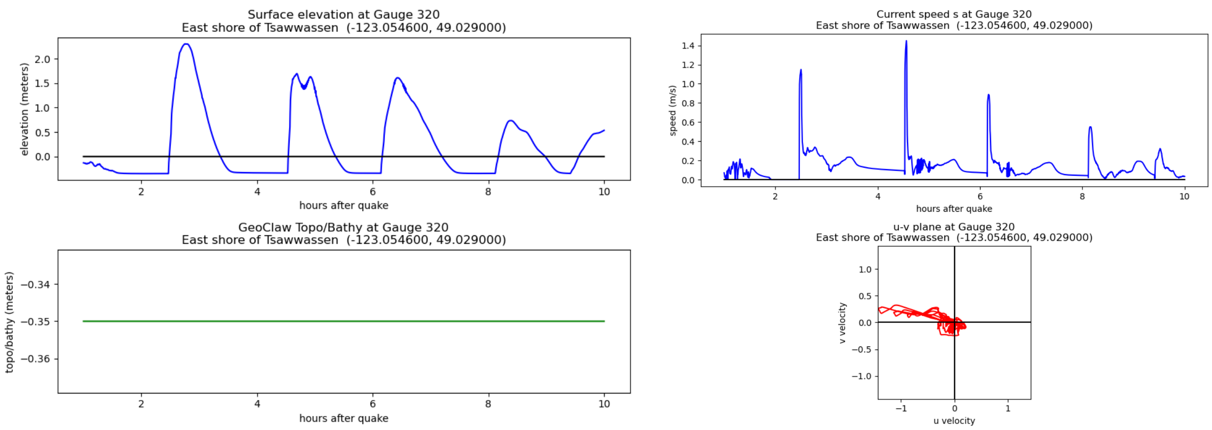

Gauge 320: East shore of Tsawwassen

Computed on region `PtRoberts`.

AKmaxWA event:

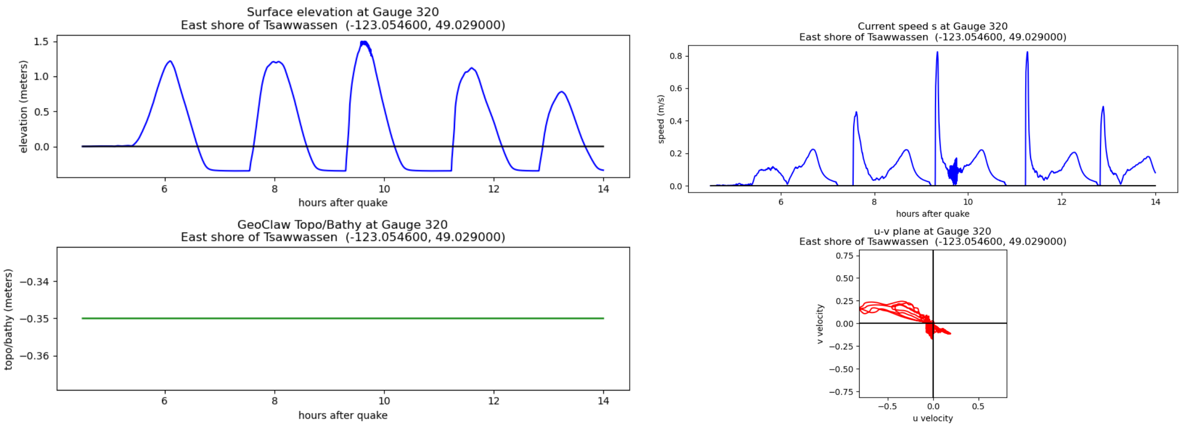

SFL event:

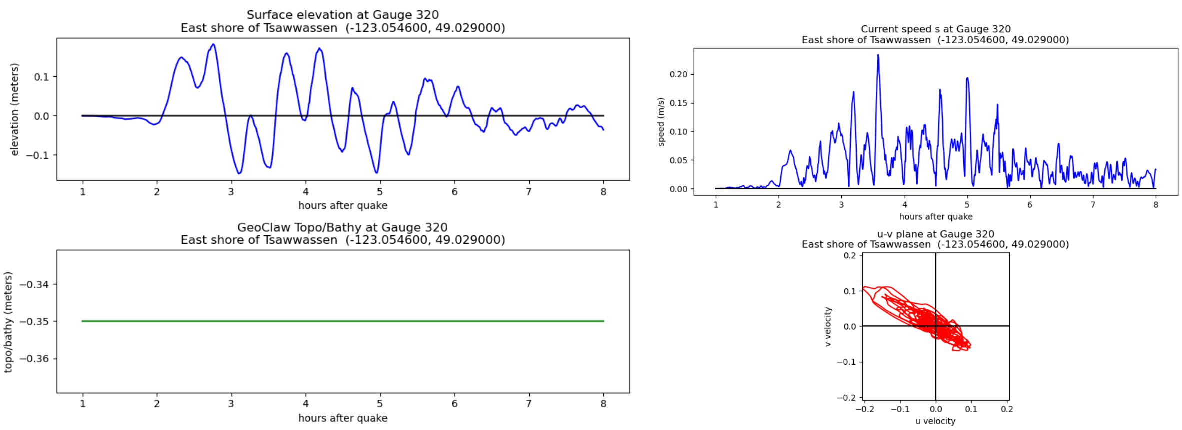

Appendices

A Data format

The deliverables described here are currently available on the Supplementary Materials website [18], which also contains additional materials and the code used to produce input data, run GeoClaw, postprocess output, and produce the plots shown in this paper and on the website. The permanently archived version is available by request from the Washington State Geological Survey.

A.1 fgmax values

For each earthquake source, output data is provided in a set of netCDF files, one for each of the regions associated with the source as listed in Table 1 and shown in Sections 6.1 and 6.2. There are two regions called `PtRoberts` and `Semiahmoo`. Four tsunami sources were considered for region `PtRoberts` and one source for region `Semiahmoo` so a total of 5 netCDF files are provided with results. The netCDF files archived have names of the form `REGION_EVENT_results.nc` where `REGION` is replaced by the fgmax region on which it was computed, and `EVENT` is replaced by the event (one of `CSZ_XL1, CSZ_L1, SFL, AK`). The AK event is also referred to as AKmaxWA and the SFL event as SF-L.

The netCDF files contain the field variables described below. Some are generated before the GeoClaw run as part of the input, and are independent of the tsunami source event, depending only on the fgmax region. Others are generated after the run from the fgmax output. Note that all variables are stored on two-dimensional uniform grids as defined by the `lon` and `lat` arrays. Only the points on this grid where `fgmax_point == 1` are used as fgmax points and only at these points is fgmax output available.

Values created as part of the GeoClaw input:

- `lon`: longitude, x (degrees),
- `lat`: latitude, y (degrees),
- `Z`: topography value Z from the DEM, relative to MHW (m),
- `fgmax_point`: 1 if this point is used as an fgmax point, 0 otherwise.
- `force_dry_init`: 0 if this point is initialized as usual, 1 if the point is forced to be dry regardless of topography.

The `force_dry_init` array was used in the `PtRoberts` region because some areas were identified as dry land below MHW behind dikes. This array was not needed in the `Semiahmoo` region.

Values created based on the GeoClaw output:

- `dz`: Co-seismic surface deformation interpolated to each point (m),
- `B`: post-seismic topography value B from GeoClaw at gauge location (m),
- `h`: maximum depth of water over simulation (m),
- `s`: maximum speed over simulation (m/s),
- `hss`: maximum momentum flux hs^2 over simulation (m^3/s^2),
- `hmin`: minimum depth of water over simulation (m),
- `arrival_time`: apparent arrival time of tsunami (s),

In addition, the netCDF files contain the following metadata values:

- `tfinal`: Final time of GeoClaw simulation (seconds),
- `history`: Record of times data was added to file,
- `outdir`: Location of output directory where data was found,
- `run_finished`: Date and time run finished,

Recall that the fgmax points are exactly aligned with the 1/3" DEM points. The finest level computational finite volume grid is also aligned so that cell centers are exactly at the fgmax points, and Z in the netCDF file is the value from the DEM at this point. However, the topography value B used in a grid cell in GeoClaw is obtained by integrating a piecewise bilinear function that interpolates the 1/3" DEM, and so B does not exactly equal Z initially. Moreover, B is the value after any co-seismic deformation associated with the event.

A.2 Gauge time series

The gauge time series was captured from each simulation every time step, but was then interpolated to 5 second increments to create the time series stored in the netCDF file for each gauge. The gauges were generally turned on only after the finest level computational grids were introduced around the fgmax region, and so time series do not start at $t = 0$ in general. All gauges were within some fgmax region and so the finest computational grid around the gauge had a resolution of 1/3". The time step then depends on the maximum depth over this region (since GeoClaw requires computing with a time step satisfying the CFL condition), but in general was less than 1 second. Gauge 301 is the same as gauge 1 in the 2018 modeling of Whatcom County. Even though the topo files used are now more complete the results are quite consistent.

The netCDF files archived have names of the form `REGION_EVENT_gauge00000.nc` where `REGION` is replaced by the fgmax region on which it was computed, `EVENT` is replaced by the event (one of `CSZ_XL1, CSZ_L1, SFL, AK`), and `00000` is replaced by the gauge number. The AK event is also referred to as AK-maxWA and event SFL as SF-L.

The netCDF files contain the following field variables:

`times`: time (seconds post-quake),
`zGeo`: post-seismic topography value B from GeoClaw at gauge location (m),
`h`: depth of water at gauge in simulation (m),
`u`: E/W velocity u at gauge (m/s),
`v`: N/S velocity v at gauge (m/s),
`level`: AMR refinement level at gauge at this time.

In addition, the netCDF files contain the following metadata values:

`history`: Record of times data was added to file,
`outdir`: Location of output directory where data was found,
`run_finished`: Date and time run finished,

B Modeling Details and GeoClaw Modifications

GeoClaw Version 5.8.0 was used for the modeling. This open source software is distributed as part of Clawpack, and is available from [8].

For this project no custom Fortran code was used, and GeoClaw from the archived Version 5.8.0 of Clawpack was used.

Summary of new Python code: The following modules, scripts, and Jupyter notebooks were used in this project. They are archived and can be viewed at [18].

In the `topo` directory:

- The notebook `topo/make_topo_files.ipynb` was used to crop and subsample the 1/9" DEMs to 1/3" and merge them into cropped versions of the SJdF and PT 1/3" DEMs.
- The notebook `make_input_files_south.ipynb` was used to pre-process DEMs and select fgmax points, define Ruled Rectangle flag regions for adaptive refinement around the fgmax points, and create kml files to view the topography.

In the `common_python` directory:

- `nc_tools.py` contains tools for reading and writing netCDF files in the formats required for this project.
- `process_fgmax.py` uses these tools for post-processing fgmax results and writing netCDF files.
- `process_gauges.py` for post-processing gauge results and writing netCDF files.

C Gauge comparisons to 2018 `N1` region in Drayton Harbor

In this appendix we present comparisons of the new results in the `Semiahmoo` region with the previous 2018 Whatcom County `N1` region at two gauges.

- Gauge 301 from the `Semiahmoo` region is the same as Gauge 1 from the `N1` region, at the entrance to Drayton Harbor.
- Gauge 361 from the `Semiahmoo` region is the same as Gauge 61 from the `N1` region, near the center of Drayton Harbor.

Recall that the 2018 results [1] used similar topography around the harbor but much poorer topography north of the border in Boundary Bay, and hence may not have captured reflected waves properly.

The comparisons in Figures 14 and 15 show that the maximum wave height and speed at the gauge locations are fairly insensitive to the modified topography, having occured with the first wave. This gives some confidence that the maximum inundation and speed results reported in the 2018 report [1] are still valid.

Later waves show more variation, particularly in the speed at Gauge 301, in the entrance to Drayton Harbor.

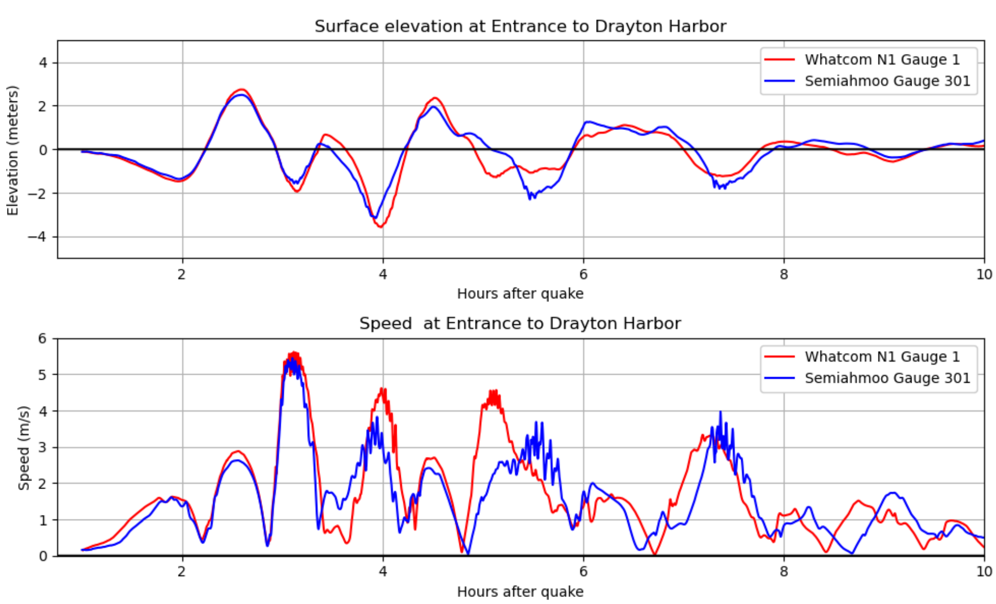

Figure 14: Comparison of modeled time series from Gauge 301 of the `Semiahmoo` region and Gauge 1 from the 2018 `N1` region, at the entrance to Drayton Harbor.

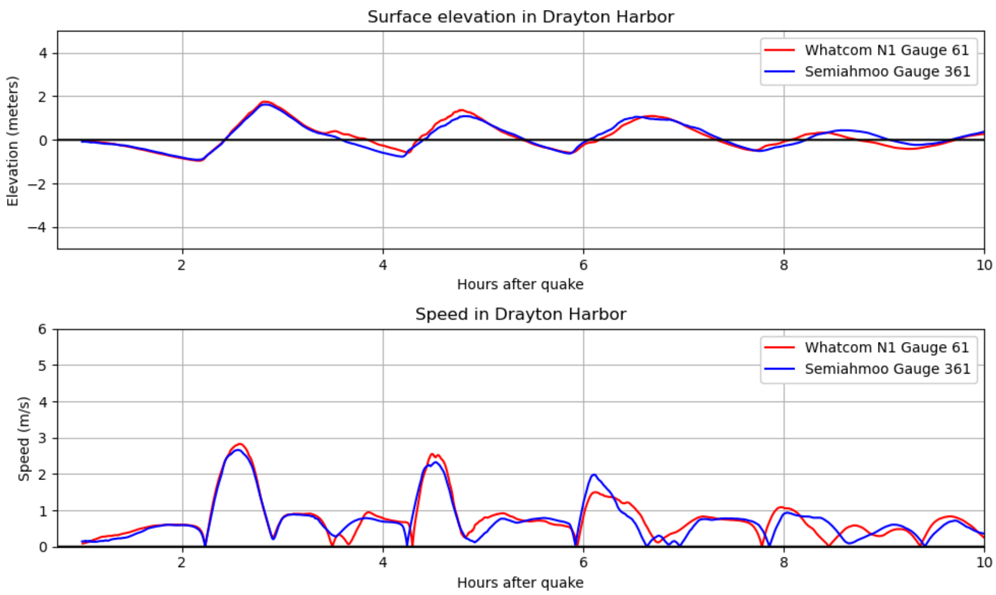

Figure 15: Comparison of modeled time series from Gauge 361 of the `Semiahmoo` region and Gauge 1 from the 2018 `N1` region, near the center of Drayton Harbor.

Acknowledgments

This work was funded by NOAA Award #NA20NWS4670068. This does not constitute an endorsement by NOAA. The earthquake deformation files for the CSZ-L1 event was provided by the NOAA Center for Tsunami Research (NCTR), PMEL, as were the unit source parameters for the AKmaxWA source. We acknowledge computing time provided in part by the Applied Mathematics Department at the University of Washington. We thank Ocean Networks Canada (ONC) and NCEI for providing pre-publication versions of the newest 1/9" DEMs used for the coastal regions of this study, which will appear at [9] and are described in [24, 26].

Data availability

The computer code and input data used in this study, along with selected GeoClaw fgmax grid and gauge output, has been archived and is available on request from the Washington State Geological Survey. Much of this data and the resulting GeoClaw output is also available on the non-archival website [18].

References

[1] L. Adams, F. González, and R. LeVeque, *Tsunami Hazard Assessment of Whatcom County, Washington, Project Report – Version 2*, 2019, http://hdl.handle.net/1773/45586.

[2] L. Adams, F. González, and R. LeVeque, *Tsunami Hazard Assessment of Island and Skagit Counties Washington, Project Report*, 2020, http://depts.washington.edu/ptha/IslandSkagitTHA_2019/.

[3] C. Amante and B. W. Eakins, *ETOPO1 1 Arc-Minute Global Relief Model: Procedures, Data Sources and Analysis.* NOAA Technical Memorandum NESDIS NGDC-24, http://www.ngdc.noaa.gov/mgg/global/global.html, 2009, https://doi.org/10.7289/V5C8276M.

[4] B. Atwater, M.-R. Satoko, K. Satake, T. Yoshinobu, U. Kazue, and D. Yamaguchi. USGS professional paper 1707, 2005.

[5] M. J. Berger, D. L. George, R. J. LeVeque, and K. T. Mandli, *The geoclaw software for depth-averaged flows with adaptive refinement.* Preprint and simulations: www.clawpack.org/links/papers/awr10, 2010.

[6] C. Chamberlin and D. Arcas, *Modeling tsunami inundation for hazard mapping at Everett, Washington, from the Seattle Fault.* OAA Technical Memorandum OAR PMEL-147, 2015, https://doi.org/10.7289/V59Z92V0, https://repository.library.noaa.gov/view/noaa/11189.

[7] C. D. Chamberlin, V. V. Titov, and D. Arcas, *Modeling tsunami inundation impact on the Washington coast from distant seismic sources.* NOAA Tech. Memo. OAR PMEL-152, 2021.

[8] Clawpack Development Team, *Clawpack software*, 2021, https://doi.org/10.5281/zenodo.4503024, http://www.clawpack.org. Version 5.8.0.

[9] Cooperative Institute for Research in Environmental Sciences, *Continuously Updated Digital Elevation Model (CUDEM) – 1/9 Arc-Second Resolution Bathymetric-Topographic Tiles.* NOAA National Centers for Environmental Information, Prepublication version provided by NCEI in 2020, https://doi.org/10.25921/ds9v-ky35.

[10] I. V. Fine and R. E. Thomson, *Numerical Simulation of a Cascadia Subduction Zone Tsunami with Application to Boundary Bay in the Southern Strait of Georgia.* Report prepared for Defence Research and Development Canadas Centre for Security Science (DRDC CSS) Program (CSSP), Coastal Flood Mitigation Canada CSSP-2018-CP-2352, 2020.

[11] I. V. Fine and R. E. Thomson, *Numerical Simulation of an Alaska 1964-Type Tsunami with Application to Boundary Bay in the Southern Strait of Georgia*. Report prepared for Defence Research and Development Canadas Centre for Security Science (DRDC CSS) Program (CSSP), Coastal Flood Mitigation Canada CSSP-2018-CP-2352, 2020.

[12] D. Gao, K. Wang, T. L. Insua, M. Sypus, M. Riedel, and T. Sun, *Defining megathrust tsunami source scenarios for northernmost Cascadia*, Natural Hazards, 94 (2018), pp. 445–469, https://doi.org/10.1007/s11069-018-3397-6.

[13] E. Gica and D. Arcas, *Tsunami Inundation Modeling of Anacortes and Bellingham, Washington due to a Cascadia Subduction Zone Earthquake*. PMEL Tech report, 2016, ftp://newportftp.pmel.noaa.gov/tsunami/WaEMD/Anacortes_Bellingham/documentation/Anacortes_Bellingham_Washington_Report.pdf.

[14] F. González, R. J. LeVeque, J. Varkovitzky, P. Chamberlain, B. Hirai, and D. L. George, *GeoClaw Results for the NTHMP Tsunami Benchmark Problems*. http://depts.washington.edu/clawpack/links/nthmp-benchmarks, 2011.

[15] R. LeVeque, L. Adams, and F. González, *Tsunami Hazard Assessment of the Strait of Juan de Fuca, Project Report*. (website containing reports and data), http://depts.washington.edu/ptha/WA_EMD_2021/.

[16] R. LeVeque, F. González, and L. Adams, *Tsunami Hazard Assessment of Snohomish County, Washington, Project Report – Version 2*, 2018, http://staff.washington.edu/rjl/pubs/THA_Snohomish.

[17] R. J. LeVeque, L. M. Adams, and F. I. González, *Tsunami Hazard Assessment of the Northwestern Coast of Washington*. (website containing reports and data), 2020, http://depts.washington.edu/ptha/WA_EMD_2020/.

[18] R. J. LeVeque, L. M. Adams, and F. I. González, *Tsunami Hazard Assessment of Point Roberts, Washington*. (website containing reports and data), 2021, http://depts.washington.edu/ptha/WA_EMD_2021_PtRoberts/.

[19] R. J. LeVeque, D. L. George, and M. J. Berger, *Tsunami modeling with adaptively refined finite volume methods*, Acta Numerica, (2011), pp. 211–289.

[20] NOAA National Geophysical Data Center, *Port Townsend 1/3 Arc-second MHW Coastal Digital Elevation Model*. https://www.ncei.noaa.gov/metadata/geoportal/rest/metadata/item/gov.noaa.ngdc.mgg.dem:366/html, Accessed 2017.

[21] NOAA National Geophysical Data Center, *Strait of Juan de Fuca 1/3 arc-second NAVD 88 Coastal Digital Elevation Model*. https://www.ncei.noaa.gov/metadata/geoportal/rest/metadata/item/gov.noaa.ngdc.mgg.dem:11514/html, Accessed 2017.

[22] NOAA National Geophysical Data Center, *British Columbia 3 arc-second Bathymetric Digital Elevation Model*. https://www.ncei.noaa.gov/metadata/geoportal/rest/metadata/item/gov.noaa.ngdc.mgg.dem:4956/html, Accessed 2018.

[23] NOAA National Geophysical Data CenterCEI, *Puget Sound 1/3 Arc-second MHW Coastal Digital Elevation Model*. https://www.ncei.noaa.gov/metadata/geoportal/rest/metadata/item/gov.noaa.ngdc.mgg.dem:5164/html, Accessed 2017.

[24] Ocean Networks Canada, *Canadian Safety and Security Program — Coastal Flood Mitigation Digital Elevation Model Workshop Report*, 2020, https://wiki.oceannetworks.ca/download/attachments/78414246/CSSP_DEM_Workshop_Report.pdf.

[25] M. D. Petersen, C. H. Cramer, and A. D. Frankel, *Simulations of Seismic Hazard for the Pacific Northwest of the United States from Earthquakes Associated with the Cascadia Subduction Zone*, Pure Appl. Geophys., 159 (2002), pp. 2147–2168.

[26] M. Rankin and A. Shumlich, *Canadian Safety and Security Program (CSSP) Coastal Flood Mitigation Canada Semiahmoo, BC Project. Milestone 2 – Digital Elevation Model (DEM) Development and Workshop*. Report submitted to Natural Resources Canada, 2020.

[27] K. Satake, K. Wang, and B. F. Atwater, *Fault slip and seismic moment of the 1700 Cascadia earthquake inferred from Japanese tsunami descriptions*, J. Geophys. Res., 108(B11) (2003), p. 2535, https://doi.org/10.1029/2003JB002521.

[28] E. Suleimani, *Numerical Studies of Tectonic and Landslide-Generated Tsunamis Caused by the 1964 Great Alaska Earthquake*, PhD thesis, University of Alaska Fairbanks, United States – Alaska, 2011, https://www.proquest.com/docview/882402282/abstract/8B0F7D434AB74405PQ/1.

[29] V. Titov, D. Arcas, C. Moore, R. LeVeque, L. Adams, and F. González, *Tsunami Hazard Assessment of Bainbridge Island, Washington, Project Report*, 2018, http://staff.washington.edu/rjl/pubs/THA_Bainbridge.

[30] R. C. Witter, Y. Zhang, K. Wang, G. Priest, C. Goldfinger, L. Stimely, J. English, and P. Ferro, *Simulating tsunami inundation for a range of Cascadia megathrust earthquake scenarios at Bandon, Oregon USA*, Geosphere, 9 (2013), pp. 1783–1803.

[31] R. C. Witter, Y. Zhang, K. Wang, G. R. Priest, C. Goldfinger, L. L. Stimely, J. T. English, and P. A. Ferro, *Simulating tsunami inundation at Bandon, Coos County, Oregon using hypothetical Cascadia and Alaska earthquake scenarios.* Oregon Department of Geology and Mineral Industries Special Paper 43, 2011.